Published in final edited form as:
J Comp Neurol. 2013 November ; 521(16): 3741–3767. doi:10.1002/cne.23376.

Neuronal and Nonneuronal Cholinergic Structures in the Mouse Gastrointestinal Tract and Spleen

Laurent Gautron[1,4,*], **Joseph M. Rutkowski**[1,3], **Michael D. Burton**[1,4], **Wei Wei**[2], **Yihong Wan**[2], and **Joel K. Elmquist**[1,4]

[1]Department of Internal Medicine, The University of Texas Southwestern Medical Center, Dallas, Texas 75235

[2]Department of Pharmacology, The University of Texas Southwestern Medical Center, Dallas, Texas 75235

[3]Touchstone Diabetes Center, The University of Texas Southwestern Medical Center, Dallas, Texas 75235

[4]Division of Hypothalamic Research, The University of Texas Southwestern Medical Center, Dallas, Texas 75235

Abstract

Accumulating evidence demonstrates that acetylcholine can directly modulate immune function in peripheral tissues including the spleen and gastrointestinal tract. However, the anatomical relationships between the peripheral cholinergic system and immune cells located in these lymphoid tissues remain unclear due to inherent technical difficulties with currently available neuroanatomical methods. In this study, mice with specific expression of the tdTomato fluorescent protein in choline acetyltransferase (ChAT)-expressing cells were used to label preganglionic and postganglionic cholinergic neurons and their projections to lymphoid tissues. Notably, our anatomical observations revealed an abundant innervation in the intestinal lamina propria of the entire gastrointestinal tract principally originating from cholinergic enteric neurons. The aforementioned innervation frequently approached macrophages, plasma cells, and lymphocytes located in the lamina propria and, to a lesser extent, lymphocytes in the interfollicular areas of Peyer's patches. In addition to the above innervation, we observed labeled epithelial cells in the gallbladder and lower intestines, as well as Microfold cells and T-cells within Peyer's patches. In contrast, we found only a sparse innervation in the spleen consisting of neuronal fibers of spinal origin present around arterioles and in lymphocyte-containing areas of the white pulp. Lastly, a small population of ChAT-expressing lymphocytes was identified in the spleen including both T- and B-cells. In summary, this study describes the variety of cholinergic neuronal and nonneuronal cells in a position to modulate gastrointestinal and splenic immunity in the mouse.

*CORRESPONDENCE TO: Department of Internal Medicine, The University of Texas Southwestern Medical Center, 5323 Harry Hines Blvd., Dallas, Texas 75235. laurent.gautron@utsouthwestern.edu..

CONFLICT OF INTEREST STATEMENT The authors have no identified conflict of interest.

ROLE OF AUTHORS All authors had full access to all the data in the study and take responsibility for the integrity and accuracy of the data. Study concept and supervision: L.G. and J.K.E. Acquisition and analysis of data: L.G., M.B., and J.M.R. Drafting and critical revision of the manuscript: L.G. and J.M.R. Obtained funding: J.K.E. Technical support: W.W and Y.W.

Keywords

anterograde tracing; enteric; genetic; immunity; parasympathetic

A rapidly growing area of research has identified a key role of peripheral acetylcholine in modulating immune function. For example, pharmacological administration of nicotinic receptor agonists reduces the severity of systemic endotoxemia (Pavlov et al., 2007) and various animal models of inflammation of the intestines and pancreas (Galitovskiy et al., 2011; Ghia et al., 2008; van Westerloo et al., 2005). Likewise, electrical stimulation of the efferent vagus nerve, whose primary neurotransmitter is acetylcholine, mimics the antiinflammatory actions of nicotinic receptor agonists in the above experimental models of inflammation (Borovikova et al., 2000; Meregnani et al., 2011; Mina-Osorio et al., 2012; Wang et al., 2003). In support of a direct immunomodulatory action of acetylcholine signaling in immune cells, lymphocytes and macrophages have been found to express nicotinic acetylcholine receptors (Fujii et al., 2008; Kikuchi et al., 2008; Wang et al., 2003). Notably, nicotine directly and dose-dependently reduces proinflammatory cytokines release from peritoneal and splenic macrophages (de Jonge et al., 2005; Huston et al., 2006; Wang et al., 2003). Details of the immunomodulatory role of peripheral acetylcholine are highlighted in several recent reviews (Andersson and Tracey, 2012; Ben-Horin and Chowers, 2008).

The presence of acetylcholine in the gastrointestinal tract is readily explained by its rich innervation by the vagus nerve (Berthoud et al., 1991). In addition, a large number of cholinergic enteric neurons are located in the different layers of the intestinal wall (Anlauf et al., 2003; Chiocchetti et al., 2003; Furness et al., 1985b; Mongardi Fantaguzzi et al., 2009; Rothman and Gershon, 1982; Tonini and Costa, 1990). Moreover, neuronal fibers have been described in close proximity to immune cells residing in the gut-associated lymphoid tissue (Hisajima et al., 2005; Ma et al., 2007; Shibata et al., 2008), and physiological evidence indicates that vagal and enteric neurons contribute to regulate gut immunity (Collins et al., 1992; Ghia et al., 2008; Margolis et al., 2011; Nurgali et al., 2011; Sharkey and Kroese, 2001). Nonetheless, little is known about the anatomical distribution of cholinergic neuronal fibers in relationship with the various populations of immune cells residing in the gut-associated lymphoid tissues, and the visualization of cholinergic structures in the intestines has remained technically challenging.

Unlike in the gastrointestinal tract, the presence of acetylcholine in the spleen has been difficult to demonstrate. Henry Dale biochemically isolated significant amount of acetylcholine from the bovine and equine spleen as early as 1929 (Dale and Dudley, 1929). Subsequent studies have identified acetylcholine and cholinergic markers in the cat splenic nerve (Burn and Rand, 1960; Fillenz, 1970). In contrast, others have discounted the presence of significant cholinergic innervation to the rodent spleen (Bellinger et al., 1993; Reilly et al., 1979; Schafer et al., 1998). Several studies have also established that epithelial cells and certain immune cells including splenic lymphocytes are fully capable of synthesizing and releasing acetylcholine (Fujii et al., 2008; Rinner et al., 1998; Rosas-Ballina et al., 2011; Wessler et al., 1998), suggesting that acetylcholine may be secreted by nonneuronal cell

types in various tissues. However, the presence of neuronal versus nonneuronal sources of acetylcholine-synthesizing structures in the gut-associated lymphoid tissue and spleen has not been thoroughly investigated in intact animals.

Thus, there are still numerous uncertainties regarding the neural pathways and cell types implicated in the immunomodulary actions of peripheral acetylcholine. This is in part due to the various technical limitations that make the visualization of cholinergic structures by histochemical means challenging. Cholinergic markers have been widely used to label cholinergic cells, axons, and terminals in peripheral tissues (Anlauf et al., 2003; Arvidsson et al., 1997; Bellier and Kimura, 2011; Schafer et al., 1998; Weihe et al., 1996; Yuan et al., 2005), but their lack of sensitivity has repeatedly been noted. Among other examples, the detection of cholinergic markers in the intestinal mucosa is variable in the rat (Ratcliffe et al., 1998; Schafer et al., 1998) and indicate only modest innervation in the mouse (Mongardi Fantaguzzi et al., 2009), despite the known cholinergic innervation to this tissue. In the spleen, the detection of cholinergic markers has been described as highly non-specific and highly variable by many investigators (Nance and Sanders, 2007; Stevens-Felten and Bellinger, 1997; Thayer and Sternberg, 2010).

Due to the aforementioned technical difficulties, we hypothesized that the detailed organization of the cholinergic innervation to the gut-associated lymphoid tissue and spleen deserves reexamination. Towards this goal, we have undertaken a series of studies using a new neural tract tracing methodology. We sought to use the Cre-LoxP technology to specifically label all choline acetyltransferase (ChAT)-expressing cells by using mice with Cre-recombinase expression under control of the endogenous ChAT promoter (Rossi et al., 2011). Specifically, we crossed the mice with a tdTomato reporter line, and ChAT-Cre-tdTomato mice were used to label the cholinergic innervation and nonneuronal acetylcholine-synthesizing cells encountered in the periphery without the need of tracer injection or immunohistochemical marker. This study provides insight and characterization of the precise anatomical localizations of ChAT-expressing structures and thus provides a basis for better mapping the potential immunomodulatory roles of acetylcholine in the gut and spleen.

MATERIALS AND METHODS

Transgenic mice

ChAT-IRES-Cre transgenic mice expressing Cre recombinase under the control of the ChAT promoter have been generated and characterized (Rossi et al., 2011). ChAT-IRES-Cre mice on a C57Bl/6 genetic background were maintained in our laboratory and genotyped by using the following primers: 5′-gtttgcagaagcggtggg-3′ (M336), 5′-agatagataatgagaggctc-3′ (M337), and 5′-ccttctatcgccttcttgacg-3′ (M338). The products of the wild-type and Cre alleles were 272 bp and 350 bp, respectively. Importantly, adult Cre recombinase expression reported by green fluorescent protein (GFP) showed that these mice indeed expressed Cre recombinase eutopically within central nervous system (CNS) cholinergic sites and preganglionic autonomic neurons (Rossi et al., 2011). ChAT-IRES-Cre mice were crossed with tdTomato reporter mice from the Jackson Laboratory (stock# 007905; Bar Harbor, ME), which possess a loxP-flanked Stop cassette preventing the

expression of CAG-driven tdTomato expression. Mice homozygous for the tdTomato gene were obtained on a B6-129S6 mixed background and genotyped according to the Jackson Laboratory's instructions. We have previously used tdTomato reporter mice to efficiently trace peripheral sensory neurons in a Cre-dependent manner (Gautron et al., 2011). All the mice used in our study were young adult males carrying one ChAT-IRES-Cre allele and one loxP-Stop-loxP-tdTomato allele (ChAT-Cre-tdTomato mice). Two ChAT-IRES-Cre animals were also used as controls in our flow cytometry experiments. Animals were housed in a light-controlled (12 hours on/12 hours off; lights on at 7 A.M.) and temperature-controlled environment (21.5–22.5°C). The animals and procedures used were approved by University of Texas Southwestern Medical Center at Dallas Institutional Animal Care and Use Committees.

Histology—On the day of sacrifice, between 9 and 11A.M., mice were deeply anesthetized with chloral hydrate (500 mg/kg, i.p.) and transcardially perfused with 10% formalin. Tissues of interest were collected by using a dissecting scope. TdTomato protein native fluorescence was directly visualized in whole mounts or in cryostatcut sections (16 μm) collected on SuperFrost slides after an overnight incubation in 20% sucrose. Our samples were labeled by using the primary antibodies listed in Table 1. Sections were incubated overnight in the primary antiserum of interest in 3% normal donkey serum with 0.25% Triton X-100 in phosphate-buffered saline (PBT, pH 7.4) (Table 1). After several washes, sections were incubated in anti-rabbit Alexa Fluor 488- (Invitrogen, Carlsbad, CA, cat. A21206; 1:1,000) or anti-rat Alexa Fluor 488- (Invitrogen, cat. A11006; 1:1,000) or biotinylated anti-goat (Jackson ImmunoResearch, West Grove, PA, cat. 705-065-147; 1:1,000) secondary antibody for 1 hour at room temperature. Following the biotinylated secondary antibodies, tissue was incubated with streptavidin Alexa Fluor 488 (Invitrogen, cat. S11223; 1:1,000).

All our samples were coverslipped with Vectashield mounting medium with 4,6-diamidino-2-phenylindole (DAPI; Vector, Burlingame, CA, H-1500). For immunoperoxidase staining, brain sections were pretreated with 1% hydrogen peroxide in PBS for 10 minutes at room temperature. Sections were incubated overnight in the anti-DsRed primary antiserum in PBT (1:2,000) followed by biotinylated donkey anti-rabbit (Jackson ImmunoResearch, cat. #711065152; lot #81161), and then incubated in a solution of ABC (Vectastain Elite ABC Kit; Vector; 1:1,000) dissolved in PBS for 1 hour. After washing in PBS, the sections were incubated in a solution of 0.04% diaminobenzidine tetrahydrochloride (DAB, Sigma, St. Louis, MO) and 0.01% hydrogen peroxide (Sigma). DAB-labeled sections were mounted on gelatin-coated slides, air-dried, dehydrated in graded ethanols, cleared in xylenes, and coverslipped with Permaslip (Alban Scientific, St. Louis, MO). A total of six and three ChAT-Cre-tdTomato mice were used for our mapping and double-labeling experiments, respectively.

Antibody characterization

The antisera used in immunohistochemistry in this study are all commercially available and their sources and dilutions are indicated in Table 1.

1. The rat monoclonal anti-mouse CD3 purified (also known as CD3 epsilon) reacts with the mouse CD3 complex. CD3 is expressed by all mature T-cells. This antibody has been tested by manufacturer by flow cytometric analysis of mouse thymocyte and splenocyte suspensions (manufacturer's datasheet). The production of the 17A2 clone has been described in the past (Miescher et al., 1989), and antibodies derived from this clone have been widely used for staining T-cells in many studies (Chaimowitz et al., 2011; Talay et al., 2012). This particular antibody was used for flow cytometric analysis and immunolabeling of T-cells in the mouse skin (Zhang et al., 2002). In accordance with previous works (Lloyd et al., 2008; Ma et al., 2007; Ward et al., 2006), this antibody labeled the cell surface of small round cells packed in the lamina propria, Peyer's patches, and spleen periarteriolar areas. Finally, western blot analysis using nonreducing conditions showed the presence of a band of approximately 25 kDa in murine T-cell lysates (Schuchert et al., 2000).

2. Goat antiserum against ChAT. Briefly, the antiserum recognizes a single band of 68–70 kDa on western blots of rat peripheral nerves (Brunelli et al., 2005) and mouse brain lysates (manufacturer's datasheet). The staining pattern obtained in this study was identical to that reported previously to stain enteric neurons (Gautron et al., 2010; Miampamba et al., 2002; Schicho et al., 2001) and perfectly coincided with the native red fluorescence of tdTomato.

3. The rat anti-human/mouse CD45R/B220 antibody reacts with the exon A-restricted isoform of mouse CD45R, a 220-kDa surface molecule. The CD45R epitope is mainly expressed by the B-cell lineage. This antibody was previously used for flow sorting of B-cells in many publications (manufacturer's datasheet). It also detects a single band of 220 kDa in murine splenocyte and thymocyte lysates (Oka et al., 2000). The staining pattern obtained with this antibody in the murine spleen (Rahman et al., 2010; Schuhmann et al., 2005) is in conformity with that obtained with other monoclonal antibodies produced from the same clone (Chaimowitz et al., 2011; Rehg et al., 2012; Talay et al., 2012) or different clones (Ward et al., 2006). In our samples, CD45R-labeled cells in the mouse spleen showed the expected shape and distribution.

4. The monoclonal rat anti-mouse F4/80 antibody recognizes the murine F4/80 antigen, a 160-kDa cell surface glycoprotein that is a marker of a wide range of mature tissue macrophages. This antibody was widely used in the past for flow sorting, imunohisto-chemistry, and western blot in the mouse (see manufacturer's datasheet). This antibody detects one large band of approximately 160 kDa in samples of peritoneal macrophages, lymphoid tissues, and skin (Hemmi et al., 2009; Moore et al., 2000; Seitz et al., 2010). Among many examples, macrophages located in the gut lamina propria, Peyer's patches, liver, and spleen are stained by this antibody (deSchoolmeester et al., 2009; Donaldson et al., 2012; Lloyd et al., 2008). The shape and localization of the cells stained in our samples are consistent with that described in the above publications. Of note, this antibody is also listed in the *Journal of Comparative Neurology* database for its application in neural tissues (Santos et al., 2010).

5. The goat anti-mouse IgA (α-chain specific) reacts with the heavy chain of mouse IgA as demonstrated by enzyme-linked immunosorbent assay (ELISA) and flow cytometry (manufacturer's datasheet). This antibody was commonly used for various applications including detecting IgA levels in the supernatant of murine IgA-secreting cells (Mora et al., 2006), as well as flow sorting and labeling of plasma cells (Obata et al., 2010; Shibata et al., 2008; Wang et al., 2004). As attested by the above publications, the staining pattern obtained in murine intestines with this antibody replicated well that obtained with other antisera (Fritz et al., 2012). Labeled cells in our samples showed the expected distribution and shape.

6. The antibody against the mouse Podoplanin (PDL) detects the mouse Podoplanin in direct ELISAs and wWestern blots (manufacturer's datasheet). Podoplanin is a mucin-type transmembrane glycoprotein with extensive O-glycosylation expressed by lymphatic endothelial cells but not blood vascular endothelial cells, as well as osteocytes and podocytes. The manufacturer tested this antibody with the recombinant mouse Podoplanin Fc Chimera (cat. 3244-PL). The Fc Chimera ran at 45–70 kDa under reducing conditions. Zhu et al. (2011) tested mouse osteoblast cell lysates and reported seeing a band at 38–40 kDa under nonreducing conditions. The staining pattern of podoplanin-positive lymph vessels in the murine intestines is well known (Backhed et al., 2007; Kajiya et al., 2005).

7. The rabbit polyclonal antiserum against tyrosine hydroxylase (TH) was previously described in several publications in the *Journal of Comparative Neurology* to label TH-containing neurons in the rodent central and peripheral nervous systems (Gautron et al., 2010; Kaufling et al., 2009). The antiserum produced intense staining of sympathetic fibers directly comparable to that obtained by Anderson and colleagues (2007) or by others using different antibodies (Phillips and Powley, 2007). The antiserum detects a single band at 62 kDa in PC12 lysates (manufacturer's datasheet).

8. The rabbit polyclonal antiserum recognized DsRed. TdTomato is a red fluorescent dimer derived from a monomeric mutant of DsRed. This antiserum detects a single 29.5-kDa band in HEK-293 cells transfected with a pDsRed-Monomer-N1 vector (ClonTech's, Palo Alto, CA, datasheet). In HEK-293 cells transfected with a vector expressing tdTomato, the antibody detects one single band of 58 kDa. By using this antibody, we detected a single band of about 58 kDa in the mouse intestines of ChAT-Cre-tdTomato mice (see Fig. 5). Moreover, the staining obtained with the DsRed antibody perfectly colocalized with the native red fluorescence of tdTomato, hence demonstrating specificity.

Western blot

By using a standard protocol (Gallagher, 2008), proteins were extracted by homogenizing duodenum samples in lysis buffer, resolved by sodium dodecyl sulfate–polyacrylamide gel electrophoresis (SDS-PAGE), and then transferred to a nitrocellulose membrane by electroblotting (30 V overnight at 4°C). TdTomato was detected by using rabbit polyclonal anti-DsRed antibody (1:1,000) incubated overnight at 4°C (Table 1), followed by anti-rabbit

Alexa Fluor 488 described earlier. β-Actin, used as loading control, was detected with a mouse monoclonal antiserum (1:5,000; Sigma, cat. A5316), followed by anti-mouse secondary antibodies goat anti-mouse IRDye 680 (Odyssey 92632220, LICOR, Lincoln, NE; 1:10,000). A total of three ChAT-Cre-tdTomato samples were used for western blot.

Flow cytometry

Spleens were removed from three ChAT-CretdTomato and ChAT-IRES-Cre (controls for fluorescence) mice at sacrifice and sliced lengthwise so as to utilize half. After a brief rinse in ice-cold PBS, spleens were minced and incubated at 37°C with Liberase enzyme (Roche, Indianapolis, IN) 1:10 in 0.5% bovine serum albumin (BSA). EDTA was added after 20 minutes to quench the digestion, and the spleens were muddled and passed through 40-μm cell strainers (Fisher Scientific, Fair Lawn, NJ) with rinsing. Red blood cells were removed by lysis with ammonium chloride lysis buffer. Approximately 2 million splenocytes were aliquoted for each cytometry sample and maintained in cold 0.5% BSA. Antibodies against B220 (Table 1) and CD11b (fluorescein isothiocyanate [FITC]-conjugated, rat anti-mouse monoclonal, 1:100, eBioscience cat.11-0112, clone M1/70) were used to identify B-cells and macrophages, respectively. An FITC-conjugated rat anti-mouse CD19 (1:500, eBioscience, San Diego, Ca, cat.11-0191, clone MB19-1) was also used to confirm B-cell populations, and a CD3 antibody (Table 1) for T-cells. The antibodies were previously widely used in the past for flow cytometry analysis of splenic immune cells (manufacturer's datasheet). DAPI was applied to the cells before flow cytometry analysis to exclude dead or dying cell populations.

Cell population identifications were performed on a Dako (Carpinteria, CA) CyAnalyzer flow cytometer (flow cytometry core at UTSouthwestern) with fluorescence compensation applied to all channels equivalently for all samples. Populations were analyzed by using FlowJo software (Tree Star, Ashland OR) for living single cells, divided into B220+/CD19+ and CD3e+/CD19− populations that were then assessed for the percentage of tdTomato-positive cells. Finally, we used quantitative polymerase chain reaction (qPCR) to demonstrate the enrichment of ChAT mRNA in splenic flow-sorted tdTomato-positive versus tdTomato-negative cells. ChAT was never detected in samples containing negative cells but was present at low levels (Ct ~35) in three samples containing about 6,000 Tomato-positive cells (not shown). Hence, we are confident that ChAT was truly expressed, albeit at a low level, in tdTomato-positive lymphocytes.

Benzalkonium chloride denervation

The focal denervation of the intestines was conducted following previous protocols (Hanani et al., 2003; Parr and Sharkey, 1997). Briefly, mice were anesthetized with ketamine HCl/xylazine HCl (80:12 mg/kg, i.p.), their abdomens were opened longitudinally under aseptic conditions, and the duodenum was exposed. A piece of gauze (~1 cm long) soaked in benzalkonium chloride (BAC; Sigma-Aldrich, St. Louis, MO, cat. 234427, lot. 141801; 0.1% in 0.9% sterile saline) was gently applied onto the serosal surface of the intestines about 2 cm below the pylorus for 15 minutes. Then, the BAC-treated segment was carefully rinsed with saline, and the peritoneal cavity was closed with sutures. Animals were allowed to survive for 12 days after surgery, and the treatment was without any apparent ill effects

on the animals. During sacrifice, BAC-treated segments were grossly identifiable by marked swelling. Three ChAT-Cre-tdTomato mice were BAC-treated.

Microscopy and image analysis

Images were captured by using a Zeiss microscope (Imager ZI) equipped with a scanning stage and attached to the ApoTome system and a digital camera (Axiocam MRm). Briefly, the Apotome module (structured illumination) was applied to produce confocal-like images, and the MosaiX module allowed us to automatically scan large specimens in the X-, Y- and Z-axes. In some instances, the 4D module of Axiovision 4.5 was also used to reconstruct neuroimmune proximity in three dimensions. Axiovision 4.5 was also used to stitch digital images together. The magnification, number of optical sections, and Z-step are systematically indicated in legends. When appropriate, the number of tiles (MosaiX module) and type of preparation (whole mount vs. cryosection) are also indicated. DAB staining was viewed by using a Zeiss microscope (Axioskop2).

The relative abundance of fluorescently labeled neuronal fibers and nonneuronal cells in selected tissues was evaluated by considering the number of td-Tomato–containing fibers or cell bodies by using the following density scale: +++, high density; ++, moderate density; +, low density; –, absence of fluorescence. This survey was manually performed on 16-μm sections (magnification ranging from 5× to 63×) in three mice.

The image editing software Adobe Photoshop CS2 was used to combine drawings and digital images into plates and make annotations. The contrast and brightness of images were adjusted when necessary. In addition, red–green fluorescence images were converted to magenta–green for color blind readers. In some instances, DAPI-counterstained nuclei and tdTomato fluorescent images were converted to white to achieve a better contrast.

RESULTS

Validation of ChAT-Cre-tdTomato mice as a reliable model for labeling cholinergic structures

Major classes of cholinergic autonomic neurons and projection patterns— ChAT-Cre-tdTomato mice displayed intense fluorescence in the cell bodies of autonomic cholinergic neurons (Fig. 1). This included parasympathetic preganglionic neurons in the dorsal nucleus of the vagus nerve (Fig. 1A). Parasympathetic postganglionic neurons with a cholinergic phenotype were also labeled including many enteric neurons in the gastrointestinal myenteric plexus (Fig. 1B), as well as pancreatic and gallbladder postganglionic neurons among other examples (Fig. 1C,D). Notably, fluorescence was not seen in peripheral ganglia known not to contain cholinergic neurons such as the dorsal root ganglion (Fig. 1E). We were also able to identify cholinergic neurons in the spinal cord such as motoneurons of the somatic nervous system and sympathetic preganglionic neurons in the intermediolateral column (Fig. 1F). In contrast, sparse fluorescently labeled neurons were found in autonomic ganglia containing sympathetic postganglionic neurons such as the superior cervical ganglion (Fig. 1G). Only a small subset of sympathetic postganglionic neurons are cholinergic (Elfvin et al., 1993; Schafer et al., 1997).

Notably, the tdTomato fluorescent protein was efficiently transported from the cell bodies of the aforementioned neurons to their axons and terminal endings in the periphery. As a result, abundant cholinergic innervation could be visualized throughout thoracic and abdominal viscera including the gastrointestinal tract, many endocrine and metabolic tissues, and blood vessels (Figs. 2,3, Table 2). We surveyed a few selected organs in order to assess and verify that the overall innervation patterns seen in the Chat-Cre-tdTomato mice is in accord with the literature on the anatomy of the autonomic and enteric nervous systems (Berthoud et al., 1990; Elfvin et al., 1993; Furness, 2006; Gershon, 1981; Gibbins and Morris, 2000; Powley, 2000). Among other examples, the airways and pancreas received abundant nerve supply (Fig. 2A,B). In addition, sympathetic preganglionic neurons innervated the paravertebral chain and prevertebral ganglia. For instance, a rich supply of fluorescent fibers was seen in the inferior mesenteric ganglionic complex (Fig. 2C). Sympathetic preganglionic neurons do not directly innervate internal organs with the well-known exception of the adrenal gland.

We found that the adrenal medulla contained a rich network of varicose fibers (Fig. 2D). Moreover, large blood vessels throughout the body (more often arteries than veins) contained innervation (Fig. 2E, Table 2). Thick zigzagging axons were seen wandering in the advential layers of the aorta, portal vein, skin arteries, and various mesenteric blood vessels (Fig. 2E). The well-described innervation to the sweat gland (not shown) and neuromuscular junctions was also identified (Fig. 2F). Lastly, tissues not innervated by cholinergic neurons were devoid of fluorescence including the adipose tissue (white and brown) and the testis (Table 2).

Colocalization with ChAT and TH—ChAT-Cre-tdTomato mice contained fluorescently labeled enteric cholinergic neurons located in the myenteric and submucosal plexuses of the entire gastrointestinal tract. Figure 3 shows representative labeling of the different plexuses of the distal ileum and their projections to the adjacent smooth muscle layers and (Fig. 3A,B). The patterning of labeling in the ChAT-Cre-tdTomato mice suggested that Cre-recombinase activity (as reflected by fluorescence) was restricted to neurons with a cholinergic phenotype. Double-staining experiments further established that the observed fluorescence was restricted to enteric ChAT-expressing neurons (Fig. 4). Although TH-immunoreactive fibers often traveled along with tdTomato-containing fibers in the stomach wall (Fig. 4A–D), tdTomato fluorescence never colocalized with TH immunoreactivity. In contrast, ChAT immunoreactivity was found in both preganglionic terminal endings and cell bodies of myenteric tdTomato-containing neurons (Fig. 4E–G). Notably, ChAT immunolabeling resulted in a punctuated staining and, overall, revealed less anatomical details than the native tdTomato fluorescence (Fig. 4E–J). Hence, our data suggest that cholinergic enteric neurons can be specifically labeled in an effective and reliable manner by using a genetic tracer approach.

TdTomato immunostaining—In order to improve the detection of tdTomato-containing structures, an antibody against DsRed was characterized by western blot analysis and immunohistochemistry (Fig. 5). Immunoblot of samples from the small intestines of ChAT-Cre-tdTomato revealed a single band of about 58 kDa corresponding to tdTomato (Fig. 5A). In addition, the same antibody stained tdTomato-containing structures in the following a

pattern exactly identical to the native fluorescence of the tdTomato (Fig. 5B,C), thus showing that the anti-DsRed antibody is specific and suitable for the labeling of tdTomato. In most instances, immunolabeling was not necessary to detect tdTomato. It was only used to slightly enhance the stability and brightness of the fluorescent signal at higher magnification (40× and 63×). Immunohistochemistry was also performed on adjacent series of sections by using a peroxidase technique and resulted in the permanent labeling of tdTomato-containing fibers in the intestines (Fig. 5D).

Gut-associated lymphoid tissue

Lamina propria—The intestinal mucosa was richly innervated (Fig. 6A, Table 2). This innervation was comprised of individual fibers running in the submucosa and lamina propria along the axis of each individual villus (Fig. 6A,B). Smaller branches wandered near the epithelial basal laminae (Fig. 6A,B) and often became more varicose within the tip of villi (Fig. 6A,B). We delineated the lamina propria by using a marker for lymphatic vessels (Fig. 6C). Cholinergic fibers were running along these vessels and formed an intermingled network of lymphatic capillaries and neuronal fibers. Although the intestinal lamina propria itself did not contain ChAT-expressing cells, isolated epithelial intestinal cells were sometimes fluorescent, more frequently in the distal than the proximal intestine (Fig. 6D). These cells resembled absorptive enterocytes and Brush cells (Gerbe et al., 2012), although further studies are warranted to confirm their phenotype. Notably, mucosal fibers were almost entirely eliminated following a focal chemical ablation of the enteric nervous system (Fig. 7). As described in previous works (Hanani et al., 2003; Parr and Sharkey, 1997), the application of BAC at the surface of a portion of the duodenum wall resulted in its swelling due to the disappearance of the extrinsic innervation and myenteric neurons at the site of application (Fig. 7A–E), although most submucosal neurons were spared by the treatment (Fig. 7C). The above observations combined with the predicted enteric origin (principally myenteric) of the observed mucosal innervation.

The intestinal lamina propria contains a variety of immune cells including macrophages, plasma cells, and T-cells, which all play critical roles in gut immunity (Cheroutre and Madakamutil, 2004; Hooper and Macpherson, 2010; Macdonald and Monteleone, 2005). The labeling of these populations of immune cells revealed the close proximity of gut immune cells and nearby neuronal fibers (Fig. 8A–D). Often, although no specialized neuronal endings were readily discernible onto immune cells, varicose fibers approached individual immune cells closely in proximity of less than 1 μm (Fig. 8C,E,F). We noticed that all three types of immune cells examined were in close proximity to enteric fibers in the entire length of the intestine within crypts and villi. These data support the model of paracrine action of acetylcholine on gut immune cells (see Discussion).

Peyer's patches—Peyer's patches are part of the gut-associated lymphoid tissue and play a pivotal role in antigen-presenting functions (Lelouard et al., 2012). However, the innervation of Peyer's patches is not well described. We found patterns of innervation suggesting that Peyer's patches contain a unique combination of neuronal and nonneuronal cholinergic elements (Fig. 9, Table 2). Innervation was absent from follicle and dome areas, but was consistently seen within the interfollicular area where high-endothelial vessels and

many lymphocytes are contained (Fig. 9A,D). Additionally, follicles and interfollicular areas contained a few fluorescent cells resembling lymphocytes and often positive for CD3, a marker for T-cells (Fig. 9C,E,F). Very few B-cells, identified by B220-immunofluorescence or CD19 flow cytometry, were tdTomato positive (not shown). Lastly, fluorescent M cells (Microfold cells) could be seen, easily recognized by their basolateral pocket-like shape and localization at the top of the dome (Fig. 9A,B).

Gallbladder—Although the gallbladder is not typically considered part of the gut-associated tissue, we sought to investigate the gallbladder for the following reasons: 1) the biliary tract is anatomically connected to the gastrointestinal lumen; 2) the gallbladder receives both an extrinsic and intrinsic cholinergic supply (Mawe, 1998); and 3) the gallbladder epithelium participates in local immune functions (Maurer et al., 2009). As anticipated, the gallbladder was innervated by preganglionic fibers terminating in small clusters of postganglionic neurons scattered in the smooth muscle (Figs. 1, 10A). These neurons then innervated the gallbladder vasculature and adjacent smooth muscle layers (Fig. 10A). In contrast, the gallbladder lamina propria was not innervated (Fig. 10B). Interestingly, the gallbladder epithelium contained many interspersed fluorescent cells with a unique topography and morphology reminiscent of that of brush cells (Fig. 10B,C). In accordance with the literature (Luciano and Reale, 1997), these putative brush cells, preferentially concentrated in the lower half of the gallbladder, displayed a bulky cell body with a slight apical protrusion, and harbored a thin basal branch (Fig. 10B,C).

Spleen

Overall, the spleen demonstrated only a modest innervation (Fig. 11, Table 2). A few individual neuronal fibers were routinely seen both around arterioles and not in association with the vasculature, wandering into lymphocyte-containing areas of the white pulp (Fig. 11A,B,E). Even though the observed fluorescent fibers never contained TH immunoreactivity, they often traveled in close apposition to TH-positive fibers, especially around arterioles (Fig. 11B–D). Of note, T-lymphocytes in the white pulp could be observed in close proximity to the latter fluorescent fibers (Fig. 11E).

Fluorescently labeled immune cells were clearly visible in the spleen of ChAT-Cre-tdTomato mice (Figs. 11,12). They were cells resembling lymphocytes located principally in the white pulp, both in the periarterial lymphoid sheaths and adjacent B-cell areas (Figs. 11A, 12A–C). These immune cells were generally not in close apposition with either TH- or tdTomato-positive fibers (Fig. 11A,D). The observed immune cells were not often positive for CD3 and never for F4/80 (Fig. 12A,B) by immunofluorescence, but frequently displayed a CD45R-positive cell surface outline (Fig. 12D–F), suggesting a novel B-cell population. Flow cytometry analysis largely corroborated our histology and allowed us to identify tdTomato-positive leukocytes with markers against B- and T-cells in unchallenged mice (Fig. 13). Specifically, it confirmed that splenic tdTomato cells belonged to a B- and T-cell lineage (Fig. 13A,B), although B-cells were more abundant. There were no tdTomato-positive cells in the spleen of ChAT-Cre animals (not shown).

DISCUSSION

This study used ChAT-Cre-tdTomato mice to examine the anatomy of the peripheral cholinergic system and its relationship with immune cells located in the gut-associated lymphoid tissue and in the spleen. Specifically, our observations revealed that: 1) macrophages, plasma cells, and T cells in the intestinal mucosa were in close proximity to a dense network of cholinergic fibers of enteric origin; 2) cholinergic epithelial and T-cells populated the gut-associated lymphoid tissue and gallbladder; and 3) the spleen contained a novel population of cholinergic B-cells, fewer T-cells, and neuronal fibers of spinal origin that closely approached lymphocytes in the white pulp. These data extend our understanding of cholinergic neuroimmune relationships in the mouse and are discussed below in the light of theknown antiinflammatory actions of the vagus nerve and acetylcholine.

Technical considerations

This study employed ChAT-IRES-Cre mice crossed with tdTomato reporter mice that possess a loxP-flanked Stop cassette preventing the expression of CAG-driven tdTomato expression. In ChAT-expressing neurons, however, the transcriptional termination sequence is excised allowing tdTomato production (Madisen et al., 2010; Muzumdar et al., 2007). As a result, bright fluorescence was visible in the cell bodies and projections of enteric cholinergic neurons, thus revealing the full extent of ChAT-expressing neurons innervation sites without the need of any tracer or immunohistochemical marker. Two prior studies have used ChAT-eGFP mice to label cholinergic cells (Rosas-Ballina et al., 2011; Tallini et al., 2006), but these studies did not examine gut-associated lymphoid tissues in a comprehensive manner. The present mouse model offers the advantage of allowing the reporter protein (tdTomato) to be invariably expressed under its own promoter once ChAT-Cre is expressed and recombination has occurred at any time in the life of the particular cell. Consequently, once recombination has occurred in ChAT-Cre-expressing cells, the fluorescent protein will be expressed independently of ChAT. This is important because neuronal and nonneuronal ChAT mRNA levels may be regulated under various physiological circumstances (Castell et al., 2002; Gibbs, 1996; Kawashima and Fujii, 2004). Our approach allows the reporter protein to be invariably expressed in ChAT cells regardless of ChAT expression levels. Furthermore, tdTomato is three times brighter than enhanced (e)GFP (Shaner et al., 2004) and is therefore better suited for anatomical studies of complex and fine neuronal projections as well as cholinergic cells with fluctuating ChAT expression.

Despite having many obvious advantages, our model could be criticized based on the possibility that ChAT may be expressed for a brief period during development (or in response to a particular physiological challenge) in cells that may later lose their cholinergic phenotype (Huber and Ernsberger, 2006). If true, tdTomato protein would be invariably expressed following embryonic recombination, hence resulting in the lifelong labeling of neurons that are not truly cholinergic in adult animals. However, we were able to demonstrate that fluorescently labeled neurons were immunoreactive for ChAT in the gastrointestinal tract and that fluorescent fibers never contained TH immunoreactivity. Furthermore, observations made in this work were in very good agreement with the known organization of the autonomic/enteric nervous system. Our data do not preclude the

synthesis of acetylcholine, but acetylcholine has been detected in the supernatant of mouse, human, and rat lymphocytes (Rinner et al., 1998). Although tdTomato native fluorescence is quite bright, an antiserum against DsRed can be used to label tdTomato-containing structures. Overall, ChAT-Cre-tdTomato mice are well suited for the anatomical study of peripheral cholinergic system.

Neuronal acetylcholine and intestinal immunity

In agreement with the literature (Anlauf et al., 2003; Chiocchetti et al., 2003; Furness et al., 1985a; Mongardi Fantaguzzi et al., 2009; Rothman and Gershon, 1982; Tonini and Costa, 1990), we described an abundant cholinergic innervation to the intestinal lamina propria that originated from enteric neurons. Cholinergic fibers closely approached immune cells within the gut-associated lymphoid tissue. It has been previously reported that mucosal immune cells are in close proximity to enteric nerve fibers labeled with generic neuronal markers or neuropeptides in the mouse (Hisajima et al., 2005; Ma et al., 2007; Shibata et al., 2008) and pig (Schmidt et al., 2007). However, only a few studies have shown that this anatomical proximity specifically occurs with cholinergic fibers in the pig intestines (Kulkarni-Narla et al., 1999; Schmidt et al., 2007). Of course, immunocompetent cells and autonomic/enteric nerves are also found in close proximity in other parts of the gut; for example, a recent work showed that the rat muscularis contains macrophages in close association with autonomic and enteric nerves (Phillips and Powley, 2012). Here, we demonstrated a very close proximity between identified cholinergic fibers and different types of gut immune cells including macrophages, plasma cells, and T-cells. Despite the short half-life of acetylcholine, it may therefore be possible that these varied immune cells are exposed to physiological amounts of acetylcholine released by enteric neurons.

There is biochemical evidence that gut immune cells express cholinergic receptors (Kikuchi et al., 2008) and many studies have shown that the manipulation of the vagus nerve (e.g., by electric stimulation, transection) can significantly impact gut immunity (de Jonge et al., 2005; Ghia et al., 2008; Gottwald et al., 1997; Hons et al., 2009; Luyer et al., 2005). Furthermore, cholinergic innervation to the intestinal mucosa may also regulate ion and nutrient transport across the epithelial barrier, as well as parietal cell secretion, blood flow, and epithelial cell proliferation, all of which could indirectly influence immune cell functions (Dhawan et al., 2012). It must be noted that, based on the literature (Berthoud et al., 1991), vagal efferents do not reach the intestinal lamina propria itself (or Peyer's patches), but synapse onto enteric neurons, which then innervate the lamina propria where they release acetylcholine. Thus, the role of enteric neurons in gut immunity is multifaceted. Enteric neurons respond to locally released inflammatory stimuli (Sharkey and Kroese, 2001), and anatomical and physiological evidence clearly suggests that these neurons are the ultimate effectors in the regulation of gut immunity (independently of the vagus nerve, although under its influence) (Margolis et al., 2011).

The presence of sparse cholinergic fibers in the Peyer's patches has been shown in large animals (i.e., sheep, pig) (Chiocchetti et al., 2008; Kulkarni-Narla et al., 1999; Vulchanova et al., 2007), and one study has described the innervation of murine Peyer's patches by using generic neuronal markers (Ma et al., 2007). The distribution and density of fibers seen in

these previous works is comparable to that observed in the present study. Briefly, our data demonstrated that, in sharp contrast with the neighboring lamina propria, Peyer's patches receive sparse innervation localized in interfollicular areas that contain lymphocytes and high-endothelium blood vessels, thus raising the possibility that neuronally derived acetylcholine may influence lymphocytes trafficking from Peyer's patches.

Nonneuronal sources of acetylcholine in the gut

It is becoming increasingly recognized that acetylcholine can be released by epithelial and immune cells, in addition to nerve endings (Fujii et al., 2008; Rinner et al., 1998; Tayebati et al., 2002; Wessler et al., 1998). Intestinal epithelial cells have been suggested to be a source of acetylcholine within the gut (Tallini et al., 2006; Wessler et al., 1998). Although ChAT-expressing cells were seen in the intestinal epithelium of ChAT-Cre-tdTomato and ChAT-eGFP mice (Tallini et al., 2006), these cells were relatively rare and their physiological relevance is still unclear. In contrast, the gallbladder epithelium contained many fluorescent cells. The morphology and distribution of these cells were clearly suggestive of brush cells (Luciano and Reale, 1997). In fact, brush cells in the trachea have been previously described as being cholinergic (Krasteva et al., 2011). Although the function of gallbladder brush cells is unknown, it is possible that acetylcholine released by these cells may very well play an important role in gallbladder and bile duct immunity.

Past studies have detected ChAT mRNA and protein in isolated murine, rat, and human T-cells (Kawashima and Fujii, 2004; Kawashima et al., 2007; Rinner et al., 1998; Salamone et al., 2011; Tayebati et al., 2002) and a recent work identified cholinergic T-cells in the mouse spleen and Peyer's patches (Rosas-Ballina et al., 2011). Likewise, the current data showed the presence of ChAT-expressing T-cells in the spleen and Peyer's patches. The ultimate role of immune-derived acetylcholine appears to be the suppression of proinflammatory cytokines release from macrophages (Borovikova et al., 2000). This may explain the potent antiinflammatory actions of cholinergic agonists in various inflammatory models. In addition, our data newly identified ChAT-expressing M cells, which are known to be implicated in mucosal immunity in responses to pathogen-associated molecular patterns in the intestinal lumen (Lelouard et al., 2012). Collectively, our anatomical observations underscore the abundance of the cholinergic neuroimmune associations and variety of cholinergic nonneuronal cells within gut-associated lymphoid tissue. This evidence suggests that the gut-associated lymphoid tissue may play an underestimated role in the immunodulatory actions of peripheral acetylcholine and vagus nerve stimulation. Because the gastrointestinal tract contains one of the largest masses of lymphoid tissue in the body (Brandtzaeg et al., 1989), it is tempting to predict that acetylcholine-mediated changes in gut immunity may significantly influence systemic immunity as well.

Splenic acetylcholine

A few studies have reported a vagal efferent innervation to the rodent spleen by using retrograde tracers (Buijs et al., 2008; Cailotto et al., 2012). However, these observations have been interpreted with caution because of the well-known technical difficulties associated with conventional tracing techniques and neurotropic viruses (Berthoud et al., 2006). The current study found a small supply of cholinergic fibers in the spleen of ChAT-

Cre-tdTomato mice. Spleen-projecting neurons are all contained in the celiac-suprarenal ganglia and paravertebral chain (Baron and Janig, 1988; Bratton et al., 2012; Cano et al., 2001; Nance and Burns, 1989). Although postganglionic sympathetic neurons are mostly noradrenergic, cholinergic fibers have been found in sympathetic nerves (Euler and Gaddum, 1931) and small subset of sympathetic postganglionic neurons displays a cholinergic phenotype (Elfvin et al., 1993; Schafer et al., 1997). Thus, we deduced that the cholinergic fibers found in the spleen came from cholinergic postganglionic sympathetic neurons located in the para- and/or prevertebral chains.

In the past, the noradrenergic innervation of the spleen has been well characterized and is known to induce arteriole and capsular contractions (Felten et al., 1985; Reilly, 1985). The role of cholinergic neurotransmission is less clear; however, studies have shown that application of acetylcholine modifies splenic volume and blood flow in a sympathomimetic manner in isolated spleen (Felten et al., 1985; Reilly, 1985). Recently, it was also shown that the migration and activation of B-cells in the spleen are regulated by the vagus nerve activity (Mina-Osorio et al., 2012). In our study, fluorescent fibers that we found in the spleen traveled along and often remained associated with periarteriolar TH-positive fibers, thus supporting the model of cooperative action of cholinergic and noradrenergic endings in controlling the splenic vasculature. In view of the historical role of acetylcholine as a potent vasodilator, and the relatively abundant cholinergic innervation to blood vessels seen in the current study, acetylcholine (and perhaps vagus nerve stimulation) may modulate immunity via local or systemic hemo- and lymphodynamic changes. In the past, studies have shown that autonomic nerves influence splenic immunity via blood flow (Reilly, 1985; Rogausch et al., 2003). In addition to modulating blood and lymph flow, it has been proposed that autonomic neurons endings in the spleen can directly modulate immune cell activity. This idea originally arose from morphological observations made by Felten and colleagues (Stevens-Felten and Bellinger, 1997) showing “synapse-like” contacts between noradrenergic terminals and immune cells in various lymphoid tissues (Crivellato et al., 1998; Felten et al., 1987; Stevens-Felten and Bellinger, 1997). Our study suggests that cholinergic fibers and immune cells are in very close proximity in the spleen white pulp and intestinal mucosa. Nonetheless, given the paucity of the cholinergic innervation in the spleen, further studies are warranted to establish the physiological significance of sympathetic cholinergic nerve endings in the spleen. In addition, further electron microscopy studies are warranted to establish the existence of “synapse-like” contacts between these putative cholinergic nerve endings and immune cells in the spleen.

Our experiments established that acetylcholine in the mouse spleen may derive from B- and T-cells in addition to spinal neuronal endings. Two prior studies identified small numbers of cholinergic T- and B-cells in the mouse populating the spleen and gut-associated lymphoid tissues by using flow sorting (Reardon et al., 2013; Rosas-Ballina et al., 2011). As suggested by others (Rosas-Ballina et al., 2011), the number of these lymphocytes may rapidly increase in immune-challenged animals due to the induction of ChAT expression and/or trafficking of cholinergic immune cells to the spleen where they may exert the potent antiinflammatory actions.

In summary, splenic immunity may be under the control of cholinergic lymphocytes and sympathetic endings with both a cholinergic and noradrenergic phenotype. However, it remains difficult to explain how this assembly of cholinergic structures is recruited by the electric stimulation of the efferent vagus nerve, primarily because vagal efferents do not project to the spleen and do not contact spleen-projecting sympathetic neurons (Bratton et al., 2012; Cano et al., 2001). Further studies are still critically needed to elucidate the exact neural pathway subserving neuroimmune relationships in the spleen.

CONCLUSIONS

Since Dale and Loewi first identified acetylcholine as a vagal neurotransmitter almost 100 years ago, the number of functions attributed to peripheral acetylcholine has grown considerably. In particular, the immunomodulatory actions of the cholinergic nervous system involve a complex interplay between autonomic nerves and immune cells, which is just beginning to be understood. In support of this idea, the present study underscores the abundance and variety of cholinergic neuronal and nonneuronal structures in a position to modulate immunity in the mouse. Our observations may serve as an anatomical resource for further studies aimed at elucidating the well-described immunomodulatory actions of peripheral acetylcholine.

Acknowledgments

We are grateful to Ian Gibbins (Flinders University, Adelaide, Australia) for his guidance on the dissection of peripheral ganglia. We thank Angie Bookout, Jong-Woo Sohn, Jason Anderson, and Matthew Harper (UTSouthwestern Medical Center) for their technical assistance.

Grant sponsor: National Institutes of Health; Grant numbers: P01DK08876 and RL1DK081185; Grant sponsor: American Heart Association; Grant number: 12SDG12050287.

LITERATURE CITED

Anderson G, Noorian AR, Taylor G, Anitha M, Bernhard D, Srinivasan S, Greene JG. Loss of enteric dopaminergic neurons and associated changes in colon motility in an MPTP mouse model of Parkinson's disease. Exp Neurol. 2007; 207:4–12. [PubMed: 17586496]

Andersson U, Tracey KJ. Reflex principles of immunological homeostasis. Annu Rev Immunol. 2012; 30:313–335. [PubMed: 22224768]

Anlauf M, Schafer MK, Eiden L, Weihe E. Chemical coding of the human gastrointestinal nervous system: cholinergic, VIPergic, and catecholaminergic phenotypes. J Comp Neurol. 2003; 459:90–111. [PubMed: 12629668]

Arvidsson U, Riedl M, Elde R, Meister B. Vesicular acetylcholine transporter (VAChT) protein: a novel and unique marker for cholinergic neurons in the central and peripheral nervous systems. J Comp Neurol. 1997; 378:454–467. [PubMed: 9034903]

Backhed F, Crawford PA, O'Donnell D, Gordon JI. Post-natal lymphatic partitioning from the blood vasculature in the small intestine requires fasting-induced adipose factor. Proc Natl Acad Sci U S A. 2007; 104:606–611. [PubMed: 17202268]

Baron R, Janig W. Sympathetic and afferent neurons projecting in the splenic nerve of the cat. Neurosci Lett. 1988; 94:109–113. [PubMed: 2468112]

Bellier JP, Kimura H. Peripheral type of choline acetyltransferase: biological and evolutionary implications for novel mechanisms in cholinergic system. J Chem Neuroanat. 2011; 42:225–235. [PubMed: 21382474]

Bellinger DL, Lorton D, Hamill RW, Felten SY, Felten DL. Acetylcholinesterase staining and choline acetyltransferase activity in the young adult rat spleen: lack of evidence for cholinergic innervation. Brain Behav Immun. 1993; 7:191–204. [PubMed: 8219410]

Ben-Horin S, Chowers Y. Neuroimmunology of the gut: physiology, pathology, and pharmacology. Curr Opin Pharmacol. 2008; 8:490–495. [PubMed: 18675937]

Berthoud HR, Jedrzejewska A, Powley TL. Simultaneous labeling of vagal innervation of the gut and afferent projections from the visceral forebrain with Dil injected into the dorsal vagal complex in the rat. J Comp Neurol. 1990; 301:65–79. [PubMed: 1706359]

Berthoud HR, Carlson NR, Powley TL. Topography of efferent vagal innervation of the rat gastrointestinal tract. Am J Physiol. 1991; 260:R200–207. [PubMed: 1992820]

Berthoud HR, Fox EA, Neuhuber WL. Vagaries of adipose tissue innervation. Am J Physiol Regul Integr Comp Physiol. 2006; 291:R1240–1242. [PubMed: 16857888]

Borovikova LV, Ivanova S, Zhang M, Yang H, Botchkina GI, Watkins LR, Wang H, Abumrad N, Eaton JW, Tracey KJ. Vagus nerve stimulation attenuates the systemic inflammatory response to endotoxin. Nature. 2000; 405:458–462. [PubMed: 10839541]

Brandtzaeg P, Halstensen TS, Kett K, Krajci P, Kvale D, Rognum TO, Scott H, Sollid LM. Immunobiology and immunopathology of human gut mucosa: humoral immunity and intraepithelial lymphocytes. Gastroenterology. 1989; 97:1562–1584. [PubMed: 2684725]

Bratton BO, Martelli D, McKinley MJ, Trevaks D, Anderson CR, McAllen RM. Neural regulation of inflammation: no neural connection from the vagus to splenic sympathetic neurons. Exp Physiol. 2012; 97:1180–1185. [PubMed: 22247284]

Brunelli G, Spano P, Barlati S, Guarneri B, Barbon A, Bresciani R, Pizzi M. Glutamatergic reinnervation through peripheral nerve graft dictates assembly of glutamatergic synapses at rat skeletal muscle. Proc Natl Acad Sci U S A. 2005; 102:8752–8757. [PubMed: 15937120]

Buijs RM, van der Vliet J, Garidou ML, Huitinga I, Escobar C. Spleen vagal denervation inhibits the production of antibodies to circulating antigens. PLoS One. 2008; 3:e3152. [PubMed: 18773078]

Burn JH, Rand MJ. Sympathetic postganglionic cholinergic fibres. Br J Pharmacol Chemother. 1960; 15:56–66. [PubMed: 13806187]

Cailotto C, Costes LM, van der Vliet J, van Bree SH, van Heerikhuize JJ, Buijs RM, Boeckxstaens GE. Neuroanatomical evidence demonstrating the existence of the vagal anti-inflammatory reflex in the intestine. Neurogastroenterol Motil. 2012; 24:191–200. e193. [PubMed: 22118533]

Cano G, Sved AF, Rinaman L, Rabin BS, Card JP. Characterization of the central nervous system innervation of the rat spleen using viral transneuronal tracing. J Comp Neurol. 2001; 439:1–18. [PubMed: 11579378]

Castell X, Diebler MF, Tomasi M, Bigari C, De Gois S, Berrard S, Mallet J, Israel M, Dolezal V. More than one way to toy with ChAT and VAChT. J Physiol Paris. 2002; 96:61–72. [PubMed: 11755784]

Chaimowitz NS, Martin RK, Cichy J, Gibb DR, Patil P, Kang DJ, Farnsworth J, Butcher EC, McCright B, Conrad DH. A disintegrin and metalloproteinase 10 regulates antibody production and maintenance of lymphoid architecture. J Immunol. 2011; 187:5114–5122. [PubMed: 21998451]

Cheroutre H, Madakamutil L. Acquired and natural memory T cells join forces at the mucosal front line. Nat Rev Immunol. 2004; 4:290–300. [PubMed: 15057787]

Chiocchetti R, Poole DP, Kimura H, Aimi Y, Robbins HL, Castelucci P, Furness JB. Evidence that two forms of choline acetyltransferase are differentially expressed in subclasses of enteric neurons. Cell Tissue Res. 2003; 311:11–22. [PubMed: 12483280]

Chiocchetti R, Mazzuoli G, Albanese V, Mazzoni M, Clavenzani P, Lalatta-Costerbosa G, Lucchi ML, Di Guardo G, Marruchella G, Furness JB. Anatomical evidence – for ileal Peyer's patches innervation by enteric nervous system: a potential route for prion neuroinvasion? Cell Tissue Res. 2008; 332:185–194. [PubMed: 18317812]

Collins SM, Hurst SM, Main C, Stanley E, Khan I, Blennerhassett P, Swain M. Effect of inflammation of enteric nerves. Cytokine-induced changes in neurotransmitter content and release. Ann N Y Acad Sci. 1992; 664:415–424. [PubMed: 1280933]

Crivellato E, Soldano F, Travan L, Fusaroli P, Mallardi F. Apposition of enteric nerve fibers to plasma cells and immunoblasts in the mouse small bowel. Neurosci Lett. 1998; 241:123–126. [PubMed: 9507936]

Dale HH, Dudley HW. The presence of histamine and acetylcholine in the spleen of the ox and the horse. J Physiol. 1929; 68:97–123. [PubMed: 16994063]

de Jonge WJ, van der Zanden EP, The FO, Bijlsma MF, van Westerloo DJ, Bennink RJ, Berthoud HR, Uematsu S, Akira S, van den Wijngaard RM, Boeckxstaens GE. Stimulation of the vagus nerve attenuates macrophage activation by activating the Jak2-STAT3 signaling pathway. Nat Immunol. 2005; 6:844–851. [PubMed: 16025117]

deSchoolmeester ML, Martinez-Pomares L, Gordon S, Else KJ. The mannose receptor binds *Trichuris muris* excretory/secretory proteins but is not essential for protective immunity. Immunology. 2009; 126:246–255. [PubMed: 18624733]

Dhawan S, Cailotto C, Harthoorn LF, de Jonge WJ. Cholinergic signalling in gut immunity. Life Sci. 2012; 91:1038–1042. [PubMed: 22580288]

Donaldson DS, Kobayashi A, Ohno H, Yagita H, Williams IR, Mabbott NA. M cell-depletion blocks oral prion disease pathogenesis. Mucosal Immunol. 2012; 5:216–225. [PubMed: 22294048]

Elfvin LG, Lindh B, Hokfelt T. The chemical neuroanatomy of sympathetic ganglia. Annu Rev Neurosci. 1993; 16:471–507. [PubMed: 8384808]

Euler US, Gaddum JH. Pseudomotor contractures after degeneration of the facial nerve. J Physiol. 1931; 73:54–66. [PubMed: 16994228]

Felten DL, Felten SY, Carlson SL, Olschowka JA, Livnat S. Noradrenergic and peptidergic innervation of lymphoid tissue. J Immunol. 1985; 135(2 Suppl):755s–765s. [PubMed: 2861231]

Felten DL, Ackerman KD, Wiegand SJ, Felten SY. Noradrenergic sympathetic innervation of the spleen: I. Nerve fibers associate with lymphocytes and macrophages in specific compartments of the splenic white pulp. J Neurosci Res. 1987; 18:28–36. 118–121. [PubMed: 3316680]

Fillenz M. The innervation of the cat spleen. Proc R Soc Lond B Biol Sci. 1970; 174:459–468. [PubMed: 4190056]

Fritz JH, Rojas OL, Simard N, McCarthy DD, Hapfelmeier S, Rubino S, Robertson SJ, Larijani M, Gosselin J, Ivanov II, Martin A, Casellas R, Philpott DJ, Girardin SE, McCoy KD, Macpherson AJ, Paige CJ, Gommerman JL. Acquisition of a multifunctional IgA+ plasma cell phenotype in the gut. Nature. 2012; 481:199–203. [PubMed: 22158124]

Fujii T, Takada-Takatori Y, Kawashima K. Basic and clinical aspects of non-neuronal acetylcholine: expression of an independent, non-neuronal cholinergic system in lymphocytes and its clinical significance in immunotherapy. J Pharmacol Sci. 2008; 106:186–192. [PubMed: 18285654]

Furness JB. The organisation of the autonomic nervous system: peripheral connections. Auton Neurosci. 2006; 130:1–5. [PubMed: 16798102]

Furness JB, Costa M, Gibbins IL, Llewellyn-Smith IJ, Oliver JR. Neurochemically similar myenteric and submucous neurons directly traced to the mucosa of the small intestine. Cell Tissue Res. 1985a; 241:155–163. [PubMed: 3839715]

Furness JB, Costa M, Llewellyn-Smith IJ, Murphy R, Bornstein J, Gibbins IL, Galligan JJ, Keast JR. Organization and functions of intrinsic plexuses. Nihon Heikatsukin Gakkai Zasshi. 1985b; 21(suppl):53. [PubMed: 3831529]

Galitovskiy V, Qian J, Chernyavsky AI, Marchenko S, Gindi V, Edwards RA, Grando SA. Cytokine-induced alterations of alpha7 nicotinic receptor in colonic CD4 T cells mediate dichotomous response to nicotine in murine models of Th1/Th17- versus Th2-mediated colitis. J Immunol. 2011; 187:2677–2687. [PubMed: 21784975]

Gallagher SW, Fuller SA, Hurrell JGR. Immunoblotting and Immunodetection. Curr Protoc Immunol. 2008; 83:8:10.11–18:10.28.

Gautron L, Lee C, Funahashi H, Friedman J, Lee S, Elmquist J. Melanocortin-4 receptor expression in a vagovagal circuitry involved in postprandial functions. J Comp Neurol. 2010; 518:6–24. [PubMed: 19882715]

Gautron L, Sakata I, Udit S, Zigman JM, Wood JN, Elmquist JK. Genetic tracing of Nav1.8-expressing vagal afferents in the mouse. J Comp Neurol. 2011; 519:3085–3101. [PubMed: 21618224]

Gerbe F, Legraverend C, Jay P. The intestinal epithelium tuft cells: specification and function. Cell Mol Life Sci. 2012; 69:2907–2917. [PubMed: 22527717]

Gershon MD. The enteric nervous system. Annu Rev Neurosci. 1981; 4:227–272. [PubMed: 6111979]

Ghia JE, Blennerhassett P, Collins SM. Impaired para-sympathetic function increases susceptibility to inflammatory bowel disease in a mouse model of depression. J Clin Invest. 2008; 118:2209–2218. [PubMed: 18451995]

Gibbins IL, Morris JL. Pathway specific expression of neuropeptides and autonomic control of the vasculature. Regul Pept. 2000; 93:93–107. [PubMed: 11033057]

Gibbs RB. Fluctuations in relative levels of choline acetyltransferase mRNA in different regions of the rat basal forebrain across the estrous cycle: effects of estrogen and progesterone. J Neurosci. 1996; 16:1049–1055. [PubMed: 8558233]

Gottwald T, Lhotak S, Stead RH. Effect of truncal vagotomy and capsaicin on mast cells and IgA-positive plasma cells in rat jejunal mucosa. Neurogastroenterol Motil. 1997; 9:25–32. [PubMed: 9058389]

Hanani M, Ledder O, Yutkin V, Abu-Dalu R, Huang TY, Hartig W, Vannucchi MG, Faussone-Pellegrini MS. Regeneration of myenteric plexus in the mouse colon after experimental denervation with benzalkonium chloride. J Comp Neurol. 2003; 462:315–327. [PubMed: 12794735]

Hemmi H, Idoyaga J, Suda K, Suda N, Kennedy K, Noda M, Aderem A, Steinman RM. A new triggering receptor expressed on myeloid cells (Trem) family member, Trem-like 4, binds to dead cells and is a DNAX activation protein 12-linked marker for subsets of mouse macrophages and dendritic cells. J Immunol. 2009; 182:1278–1286. [PubMed: 19155473]

Hisajima T, Kojima Y, Yamaguchi A, Goris RC, Funakoshi K. Morphological analysis of the relation between immunoglobulin A production in the small intestine and the enteric nervous system. Neurosci Lett. 2005; 381:242–246. [PubMed: 15896477]

Hons IM, Burda JE, Grider JR, Mawe GM, Sharkey KA. Alterations to enteric neural signaling underlie secretory abnormalities of the ileum in experimental colitis in the guinea pig. Am J Physiol Gastrointest Liver Physiol. 2009; 296:G717–726. [PubMed: 19221017]

Hooper LV, Macpherson AJ. Immune adaptations that maintain homeostasis with the intestinal microbiota. Nat Rev Immunol. 2010; 10:159–169. [PubMed: 20182457]

Huber K, Ernsberger U. Cholinergic differentiation occurs early in mouse sympathetic neurons and requires Phox2b. Gene Expr. 2006; 13:133–139. [PubMed: 17017126]

Huston JM, Ochani M, Rosas-Ballina M, Liao H, Ochani K, Pavlov VA, Gallowitsch-Puerta M, Ashok M, Czura CJ, Foxwell B, Tracey KJ, Ulloa L. Splenectomy inactivates the cholinergic antiinflammatory pathway during lethal endotoxemia and polymicrobial sepsis. J Exp Med. 2006; 203:1623–1628. [PubMed: 16785311]

Kajiya K, Hirakawa S, Ma B, Drinnenberg I, Detmar M. Hepatocyte growth factor promotes lymphatic vessel formation and function. EMBO J. 2005; 24:2885–2895. [PubMed: 16052207]

Kaufling J, Veinante P, Pawlowski SA, Freund-Mercier MJ, Barrot M. Afferents to the GABAergic tail of the ventral tegmental area in the rat. J Comp Neurol. 2009; 513:597–621. [PubMed: 19235223]

Kawashima K, Fujii T. Expression of non-neuronal acetylcholine in lymphocytes and its contribution to the regulation of immune function. Front Biosci. 2004; 9:2063–2085. [PubMed: 15353271]

Kawashima K, Yoshikawa K, Fujii YX, Moriwaki Y, Misawa H. Expression and function of genes encoding cholinergic components in murine immune cells. Life Sci. 2007; 80:2314–2319. [PubMed: 17383684]

Kikuchi H, Itoh J, Fukuda S. Chronic nicotine stimulation modulates the immune response of mucosal T cells to Th1-dominant pattern via nAChR by upregulation of Th1-specific transcriptional factor. Neurosci Lett. 2008; 432:217–221. [PubMed: 18248893]

Krasteva G, Canning BJ, Hartmann P, Veres TZ, Papadakis T, Muhlfeld C, Schliecker K, Tallini YN, Braun A, Hackstein H, Baal N, Weihe E, Schutz B, Kotlikoff M, Ibanez-Tallon I, Kummer W. Cholinergic chemosensory cells in the trachea regulate breathing. Proc Natl Acad Sci U S A. 2011; 108:9478–9483. [PubMed: 21606356]

Kulkarni-Narla A, Beitz AJ, Brown DR. Catecholaminergic, cholinergic and peptidergic innervation of gut-associated lymphoid tissue in porcine jejunum and ileum. Cell Tissue Res. 1999; 298:275–286. [PubMed: 10571116]

Lelouard H, Fallet M, de Bovis B, Meresse S, Gorvel JP. Peyer's patch dendritic cells sample antigens by extending dendrites through M cell-specific transcellular pores. Gastroenterology. 2012; 142:592–601. e593. [PubMed: 22155637]

Lloyd CM, Phillips AR, Cooper GJ, Dunbar PR. Three-colour fluorescence immunohistochemistry reveals the diversity of cells staining for macrophage markers in murine spleen and liver. J Immunol Methods. 2008; 334:70–81. [PubMed: 18367204]

Luciano L, Reale E. Presence of brush cells in the mouse gallbladder. Microsc Res Tech. 1997; 38:598–608. [PubMed: 9330348]

Luyer MD, Greve JW, Hadfoune M, Jacobs JA, Dejong CH, Buurman WA. Nutritional stimulation of cholecystokinin receptors inhibits inflammation via the vagus nerve. J Exp Med. 2005; 202:1023–1029. [PubMed: 16216887]

Ma B, von Wasielewski R, Lindenmaier W, Dittmar KE. Immmunohistochemical study of the blood and lymphatic vasculature and the innervation of mouse gut and gut-associated lymphoid tissue. Anat Histol Embryol. 2007; 36:62–74. [PubMed: 17266671]

Macdonald TT, Monteleone G. Immunity, inflammation, and allergy in the gut. Science. 2005; 307:1920–1925. [PubMed: 15790845]

Madisen L, Zwingman TA, Sunkin SM, Oh SW, Zariwala HA, Gu H, Ng LL, Palmiter RD, Hawrylycz MJ, Jones AR, Lein ES, Zeng H. A robust and high-throughput Cre reporting and characterization system for the whole mouse brain. Nat Neurosci. 2010; 13:133–140. [PubMed: 20023653]

Margolis KG, Stevanovic K, Karamooz N, Li ZS, Ahuja A, D'Autreaux F, Saurman V, Chalazonitis A, Gershon MD. Enteric neuronal density contributes to the severity of intestinal inflammation. Gastroenterology. 2011; 141:588–598. e581–582. [PubMed: 21635893]

Maurer KJ, Carey MC, Fox JG. Roles of infection, inflammation, and the immune system in cholesterol gallstone formation. Gastroenterology. 2009; 136:425–440. [PubMed: 19109959]

Mawe GM. Nerves and hormones interact to control gallbladder function. News Physiol Sci. 1998; 13:84–90. [PubMed: 11390768]

Meregnani J, Clarencon D, Vivier M, Peinnequin A, Mouret C, Sinniger V, Picq C, Job A, Canini F, Jacquier-Sarlin M, Bonaz B. Anti-inflammatory effect of vagus nerve stimulation in a rat model of inflammatory bowel disease. Auton Neurosci. 2011; 160:82–89. [PubMed: 21071287]

Miampamba M, Maillot C, Million M, Tache Y. Peripheral CRF activates myenteric neurons in the proximal colon through CRF(1) receptor in conscious rats. Am J Physiol Gastrointest Liver Physiol. 2002; 282:G857–865. [PubMed: 11960782]

Miescher GC, Schreyer M, MacDonald HR. Production and characterization of a rat monoclonal antibody against the murine CD3 molecular complex. Immunol Lett. 1989; 23:113–118. [PubMed: 2534389]

Mina-Osorio P, Rosas-Ballina M, Valdes-Ferrer SI, Al-Abed Y, Tracey KJ, Diamond B. Neural signaling in the spleen controls B-cell responses to blood-borne antigen. Mol Med. 2012; 18:618–627. [PubMed: 22354214]

Mongardi Fantaguzzi C, Thacker M, Chiocchetti R, Furness JB. Identification of neuron types in the submucosal ganglia of the mouse ileum. Cell Tissue Res. 2009; 336:179–189. [PubMed: 19326148]

Moore KJ, Andersson LP, Ingalls RR, Monks BG, Li R, Arnaout MA, Golenbock DT, Freeman MW. Divergent response to LPS and bacteria in CD14-deficient murine macrophages. J Immunol. 2000; 165:4272–4280. [PubMed: 11035061]

Mora JR, Iwata M, Eksteen B, Song SY, Junt T, Senman B, Otipoby KL, Yokota A, Takeuchi H, Ricciardi-Castagnoli P, Rajewsky K, Adams DH, von Andrian UH. Generation of gut-homing IgA-secreting B cells by intestinal dendritic cells. Science. 2006; 314:1157–1160. [PubMed: 17110582]

Muzumdar MD, Tasic B, Miyamichi K, Li L, Luo L. A global double-fluorescent Cre reporter mouse. Genesis. 2007; 45:593–605. [PubMed: 17868096]

Nance DM, Burns J. Innervation of the spleen in the rat: evidence for absence of afferent innervation. Brain Behav Immun. 1989; 3:281–290. [PubMed: 2611414]

Nance DM, Sanders VM. Autonomic innervation and regulation of the immune system (1987–2007). Brain Behav Immun. 2007; 21:736–745. [PubMed: 17467231]

Nurgali K, Qu Z, Hunne B, Thacker M, Pontell L, Furness JB. Morphological and functional changes in guinea-pig neurons projecting to the ileal mucosa at early stages after inflammatory damage. J Physiol. 2011; 589:325–339. [PubMed: 21098001]

Obata T, Goto Y, Kunisawa J, Sato S, Sakamoto M, Setoyama H, Matsuki T, Nonaka K, Shibata N, Gohda M, Kagiyama Y, Nochi T, Yuki Y, Fukuyama Y, Mukai A, Shinzaki S, Fujihashi K, Sasakawa C, Iijima H, Goto M, Umesaki Y, Benno Y, Kiyono H. Indigenous opportunistic bacteria inhabit mammalian gut-associated lymphoid tissues and share a mucosal antibody-mediated symbiosis. Proc Natl Acad Sci U S A. 2010; 107:7419–7424. [PubMed: 20360558]

Oka S, Mori N, Matsuyama S, Takamori Y, Kubo K. Presence of B220 within thymocytes and its expression on the cell surface during apoptosis. Immunology. 2000; 100:417–423. [PubMed: 10929067]

Parr EJ, Sharkey KA. Multiple mechanisms contribute to myenteric plexus ablation induced by benzalkonium chloride in the guinea-pig ileum. Cell Tissue Res. 1997; 289:253–264. [PubMed: 9211828]

Pavlov VA, Ochani M, Yang LH, Gallowitsch-Puerta M, Ochani K, Lin X, Levi J, Parrish WR, Rosas-Ballina M, Czura CJ, Larosa GJ, Miller EJ, Tracey KJ, Al-Abed Y. Selective alpha7-nicotinic acetylcholine receptor agonist GTS-21 improves survival in murine endotoxemia and severe sepsis. Crit Care Med. 2007; 35:1139–1144. [PubMed: 17334244]

Phillips RJ, Powley TL. Innervation of the gastrointestinal tract: patterns of aging. Auton Neurosci. 2007; 136:1–19. [PubMed: 17537681]

Phillips RJ, Powley TL. Macrophages associated with the intrinsic and extrinsic autonomic innervation of the rat gastrointestinal tract. Auton Neurosci. 2012; 169:12–27. [PubMed: 22436622]

Powley TL. Vagal input to the enteric nervous system. Gut. 2000; 47(suppl 4):iv30–32. discussion iv36. [PubMed: 11076904]

Rahman ZS, Shao WH, Khan TN, Zhen Y, Cohen PL. Impaired apoptotic cell clearance in the germinal center by Mer-deficient tingible body macrophages leads to enhanced antibody-forming cell and germinal center responses. J Immunol. 2010; 185:5859–5868. [PubMed: 20952679]

Ratcliffe EM, deSa DJ, Dixon MF, Stead RH. Choline acetyltransferase (ChAT) immunoreactivity in paraffin sections of normal and diseased intestines. J Histochem Cytochem. 1998; 46:1223–1231. [PubMed: 9774621]

Reardon C, Duncan GS, Brustle A, Brenner D, Tusche MW, Olofsson PS, Rosas-Ballina M, Tracey KJ, Mak TW. Lymphocyte-derived ACh regulates local innate but not adaptive immunity. Proc Natl Acad Sci U S A. 2013; 110:1410–1415. [PubMed: 23297238]

Rehg JE, Bush D, Ward JM. The utility of immunohistochemistry for the identification of hematopoietic and lymphoid cells in normal tissues and interpretation of proliferative and inflammatory lesions of mice and rats. Toxicol Pathol. 2012; 40:345–374. [PubMed: 22434870]

Reilly FD. Innervation and vascular pharmacodynamics of the mammalian spleen. Experientia. 1985; 41:187–192. [PubMed: 3882449]

Reilly FD, McCuskey PA, Miller ML, McCuskey RS, Meineke HA. Innervation of the periarteriolar lymphatic sheath of the spleen. Tissue Cell. 1979; 11:121–126. [PubMed: 451988]

Rinner I, Kawashima K, Schauenstein K. Rat lymphocytes produce and secrete acetylcholine in dependence of differentiation and activation. J Neuroimmunol. 1998; 81:31–37. [PubMed: 9521603]

Rogausch H, Zwingmann D, Trudewind M, del Rey A, Voigt KH, Besedovsky H. Local and systemic autonomic nervous effects on cell migration to the spleen. J Appl Physiol. 2003; 94:469–475. [PubMed: 12391126]

Rosas-Ballina M, Olofsson PS, Ochani M, Valdes-Ferrer SI, Levine YA, Reardon C, Tusche MW, Pavlov VA, Andersson U, Chavan S, Mak TW, Tracey KJ. Acetylcholine-synthesizing T cells relay neural signals in a vagus nerve circuit. Science. 2011; 334:98–101. [PubMed: 21921156]

Rossi J, Balthasar N, Olson D, Scott M, Berglund E, Lee CE, Choi MJ, Lauzon D, Lowell BB, Elmquist JK. Melanocortin-4 receptors expressed by cholinergic neurons regulate energy balance and glucose homeostasis. Cell Metab. 2011; 13:195–204. [PubMed: 21284986]

Rothman TP, Gershon MD. Phenotypic expression in the developing murine enteric nervous system. J Neurosci. 1982; 2:381–393. [PubMed: 7062117]

Salamone G, Lombardi G, Gori S, Nahmod K, Jancic C, Amaral MM, Vermeulen M, Espanol A, Sales ME, Geffner J. Cholinergic modulation of dendritic cell function. J Neuroimmunol. 2011; 236:47–56. [PubMed: 21665296]

Santos AM, Martin-Oliva D, Ferrer-Martin RM, Tassi M, Calvente R, Sierra A, Carrasco MC, Marin-Teva JL, Navascues J, Cuadros MA. Microglial response to light-induced photoreceptor degeneration in the mouse retina. J Comp Neurol. 2010; 518:477–492. [PubMed: 20020538]

Schafer MK, Schutz B, Weihe E, Eiden LE. Target-independent cholinergic differentiation in the rat sympathetic nervous system. Proc Natl Acad Sci U S A. 1997; 94:4149–4154. [PubMed: 9108120]

Schafer MK, Eiden LE, Weihe E. Cholinergic neurons and terminal fields revealed by immunohistochemistry for the vesicular acetylcholine transporter. I. Central nervous system. Neuroscience. 1998; 84:331–359. [PubMed: 9539209]

Schicho R, Schemann M, Holzer P, Lippe IT. Mucosal acid challenge activates nitrergic neurons in myenteric plexus of rat stomach. Am J Physiol Gastrointest Liver Physiol. 2001; 281:G1316–1321. [PubMed: 11668041]

Schmidt LD, Xie Y, Lyte M, Vulchanova L, Brown DR. Autonomic neurotransmitters modulate immunoglobulin A secretion in porcine colonic mucosa. J Neuroimmunol. 2007; 185:20–28. [PubMed: 17320195]

Schuchert MJ, Wright RD, Colson YL. Characterization of a newly discovered T-cell receptor beta-chain heterodimer expressed on a CD8+ bone marrow subpopulation that promotes allogeneic stem cell engraftment. Nat Med. 2000; 6:904–909. [PubMed: 10932228]

Schuhmann B, Dietrich A, Sel S, Hahn C, Klingenspor M, Lommatzsch M, Gudermann T, Braun A, Renz H, Nockher WA. A role for brain-derived neurotrophic factor in B cell development. J Neuroimmunol. 2005; 163:15–23. [PubMed: 15885304]

Seitz O, Schurmann C, Hermes N, Muller E, Pfeilschifter J, Frank S, Goren I. Wound healing in mice with high-fat diet- or ob gene-induced diabetes-obesity syndromes: a comparative study. Exp Diabetes Res. 20102010:47–69.

Shaner NC, Campbell RE, Steinbach PA, Giepmans BN, Palmer AE, Tsien RY. Improved monomeric red, orange and yellow fluorescent proteins derived from Discosoma sp. red fluorescent protein. Nat Biotechnol. 2004; 22:1567–1572. [PubMed: 15558047]

Sharkey KA, Kroese AB. Consequences of intestinal inflammation on the enteric nervous system: neuronal activation induced by inflammatory mediators. Anat Rec. 2001; 262:79–90. [PubMed: 11146431]

Shibata M, Hisajima T, Nakano M, Goris RC, Funakoshi K. Morphological relationships between peptidergic nerve fibers and immunoglobulin A-producing lymphocytes in the mouse intestine. Brain Behav Immun. 2008; 22:158–166. [PubMed: 17931829]

Stevens-Felten, SY.; Bellinger, DL. Noradrenegic and peptidergic innervation of lymphoid organs. In: Blalock, JE., editor. Neuroimmunoendocrinology. 3rd ed. Karger; Basel: 1997. p. 99-131.

Talay O, Yan D, Brightbill HD, Straney EE, Zhou M, Ladi E, Lee WP, Egen JG, Austin CD, Xu M, Wu LC. IgE(+) memory B cells and plasma cells generated through a germinal-center pathway. Nat Immunol. 2012; 13:396–404. [PubMed: 22366892]

Tallini YN, Shui B, Greene KS, Deng KY, Doran R, Fisher PJ, Zipfel W, Kotlikoff MI. BAC transgenic mice express enhanced green fluorescent protein in central and peripheral cholinergic neurons. Physiol Genomics. 2006; 27:391–397. [PubMed: 16940431]

Tayebati SK, El-Assouad D, Ricci A, Amenta F. Immunochemical and immunocytochemical characterization of cholinergic markers in human peripheral blood lymphocytes. J Neuroimmunol. 2002; 132:147–155. [PubMed: 12417445]

Thayer JF, Sternberg EM. Neural aspects of immunomodulation: focus on the vagus nerve. Brain Behav Immun. 2010; 24:1223–1228. [PubMed: 20674737]

Tonini M, Costa M. A pharmacological analysis of the neuronal circuitry involved in distension-evoked enteric excitatory reflex. Neuroscience. 1990; 38:787–795. [PubMed: 1980147]

van Westerloo DJ, Giebelen IA, Florquin S, Daalhuisen J, Bruno MJ, de Vos AF, Tracey KJ, van der Poll T. The cholinergic anti-inflammatory pathway regulates the host response during septic peritonitis. J Infect Dis. 2005; 191:2138–2148. [PubMed: 15898001]

Vulchanova L, Casey MA, Crabb GW, Kennedy WR, Brown DR. Anatomical evidence for enteric neuroimmune interactions in Peyer's patches. J Neuroimmunol. 2007; 185:64–74. [PubMed: 17363074]

Wang H, Yu M, Ochani M, Amella CA, Tanovic M, Susarla S, Li JH, Yang H, Ulloa L, Al-Abed Y, Czura CJ, Tracey KJ. Nicotinic acetylcholine receptor alpha7 subunit is an essential regulator of inflammation. Nature. 2003; 421:384–388. [PubMed: 12508119]

Wang J, Anders RA, Wu Q, Peng D, Cho JH, Sun Y, Karaliukas R, Kang HS, Turner JR, Fu YX. Dysregulated LIGHT expression on T cells mediates intestinal inflammation and contributes to IgA nephropathy. J Clin Invest. 2004; 113:826–835. [PubMed: 15067315]

Ward JM, Erexson CR, Faucette LJ, Foley JF, Dijkstra C, Cattoretti G. Immunohistochemical markers for the rodent immune system. Toxicol Pathol. 2006; 34:616–630. [PubMed: 17067947]

Weihe E, Tao-Cheng JH, Schafer MK, Erickson JD, Eiden LE. Visualization of the vesicular acetylcholine transporter in cholinergic nerve terminals and its targeting to a specific population of small synaptic vesicles. Proc Natl Acad Sci U S A. 1996; 93:3547–3552. [PubMed: 8622973]

Wessler I, Kirkpatrick CJ, Racke K. Non-neuronal acetylcholine, a locally acting molecule, widely distributed in biological systems: expression and function in humans. Pharmacol Ther. 1998; 77:59–79. [PubMed: 9500159]

Yuan PQ, Kimura H, Million M, Bellier JP, Wang L, Ohning GV, Tache Y. Central vagal stimulation activates enteric cholinergic neurons in the stomach and VIP neurons in the duodenum in conscious rats. Peptides. 2005; 26:653–664. [PubMed: 15752581]

Zhang Y, McCormick LL, Desai SR, Wu C, Gilliam AC. Murine sclerodermatous graft-versus-host disease, a model for human scleroderma: cutaneous cytokines, chemokines, and immune cell activation. J Immunol. 2002; 168:3088–3098. [PubMed: 11884483]

Zhu D, Mackenzie NC, Millan JL, Farquharson C, MacRae VE. The appearance and modulation of osteocyte marker expression during calcification of vascular smooth muscle cells. PLoS One. 2011; 6:e19595. [PubMed: 21611184]

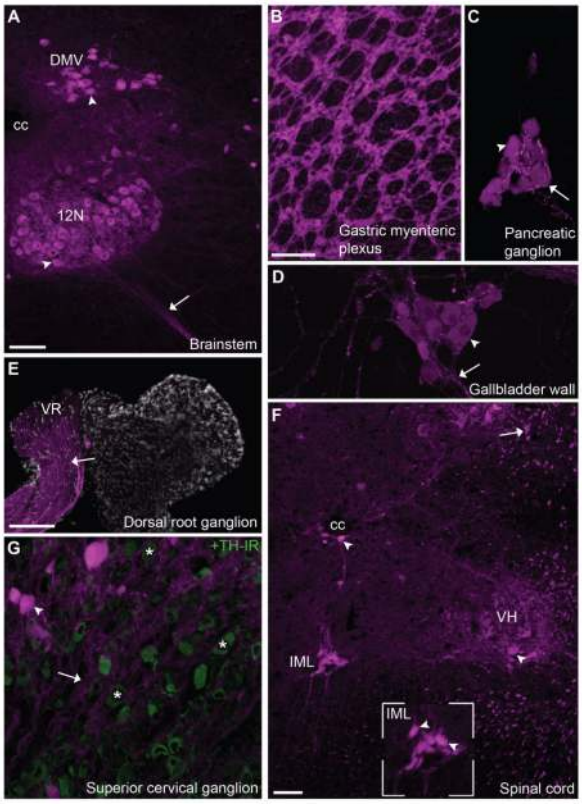

Figure 1.

Distribution of tdTomato fluorescence in autonomic cholinergic neurons of ChAT-Cre-tdTomato mice. **A:** Bright fluorescence was seen in the cell bodies of many preganglionic parasympathetic neurons in the brainstem (10×, 4 optical plans, 3- μm step). **B–D:** Postganglionic cholinergic neurons were also apparent in the (B) gastric myenteric plexus (whole mount, 5×, 5 optical plans, 32- μm step), (C) pancreatic interlobular area (20×, 10 optical plans, 1.4- μm step), and (D) gallbladder wall (20×, 10 optical plans, 1.4- μm step). **E:** In agreement with their noncholinergic phenotype, the dorsal root ganglion (along with other sensory ganglia) did not contain fluorescent neurons (5×, 3 optical plans, 2-μm step). However, cholinergic fluorescent axons originating from motoneurons were seen traveling through peripheral sensory ganglia (somatomor axons in the ventral root). **F:** Both preganglionic sympathetic neurons and somatomotor neurons were identified in coronal sections of the thoracic spinal cord (10×, 3 optical plans, 1-μm step). The inset shows representative preganglionic sympathetic neurons. **G:** Fluorescence could be discerned in a few postganglionic sympathetic in the superior cervical ganglion (20×, 3 optical plans, 2.3-μm step). The latter neurons are scattered among a vast majority of TH-positive neurons (green). Asterisks are positioned over representative TH-positive neurons. Arrows indicate fluorescently labeled neuronal individual fibers or bundle of fibers, and arrowheads point to representative cell bodies. Abbreviations: cc, central canal; DH, dorsal horn; DMV, dorsal motor nucleus of the vagus nerve; IML, intermediolateral column of the spinal cord; VH, ventral horn; 12N, hypoglossal nucleus. Scale bar = 100 μm in A; 200 μm in B (also applies to C,D,G); 50 μm in F; 200 μm in E.

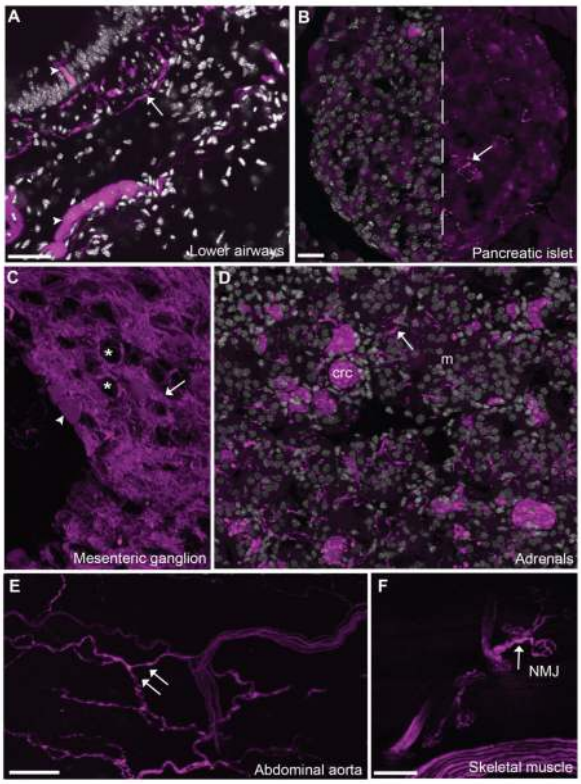

Figure 2.

Projection patterns of cholinergic neurons in selected target tissues. ChAT-expressing neurons were labeled in their entirety, thus allowing us to visualize their projections patterns in the periphery. **A:** For instance, fluorescence was seen in preganglionic parasympathetic fibers in the airways (20× 5 optical plans, 1.2-μm step). Of note, intrinsic cholinergic neurons and scattered epithelial cells were also found in the airways (arrowheads). **B:** Abundant innervation of postganglionic origin was also seen in the pancreas (20×, 6 optical plans, 1.3-μm step). **C:** Preganglionic sympathetic neurons innervated sympathetic ganglia such as the mesenteric ganglion (20×, 5 optical sections, 0.92-μm step). Asterisks are positioned over the cell profiles of putative postganglionic target neurons. As previously noted in the superior cervical ganglion, a few postganglionic sympathetic neurons appear to be cholinergic (arrowhead). **D:** The adrenals contained a large fiber supply (20×, 5 optical plans, 0.92-μm step). As a note, the fluorescence apparent in chromaffin cells corresponded to non-specific autofluorescence (seen in every filter and in wild-type animals). **E:** Although many large blood vessels throughout the body contained innervation, that of the abdominal aorta was particularly rich. **F:** The projections of cholinergic somatomotor neurons was visible as reflected by the labeling of neuromuscular junctions in the forepaw. Arrows indicate fluorescently labeled neuronal fibers, and arrowheads point to representative cell bodies. Abbreviations: crc, chromaffin cells; m, medulla; NMJ, neuromuscular junction. Scale bar = 50 μm in A; 20 μm in B (applies to B–D); 50 μm in E; 100 μm in F.

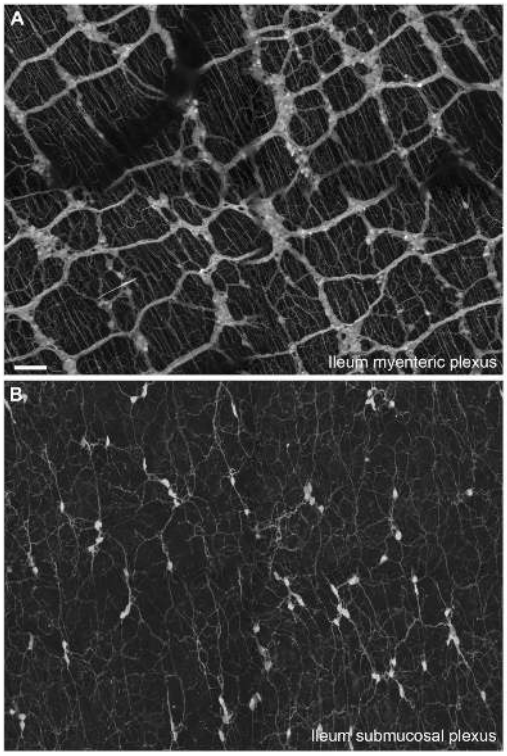

Figure 3.

Distribution of tdTomato fluorescence in ileal enteric neurons. **A:** Bright fluorescence was seen in vagal preganglionic fibers projecting to the myenteric plexus as well as numerous, but not all, enteric neurons (whole mount, 10×, 14 optical plans, 2.8-μm step, 4 tiles). Of note, projections from the enteric neurons were seen ramifying into the adjacent smooth muscle layers. **B:** Likewise, submucosal neurons and their projections and clearly labeled. Scale bar = 100 μm in A (also applies to B).

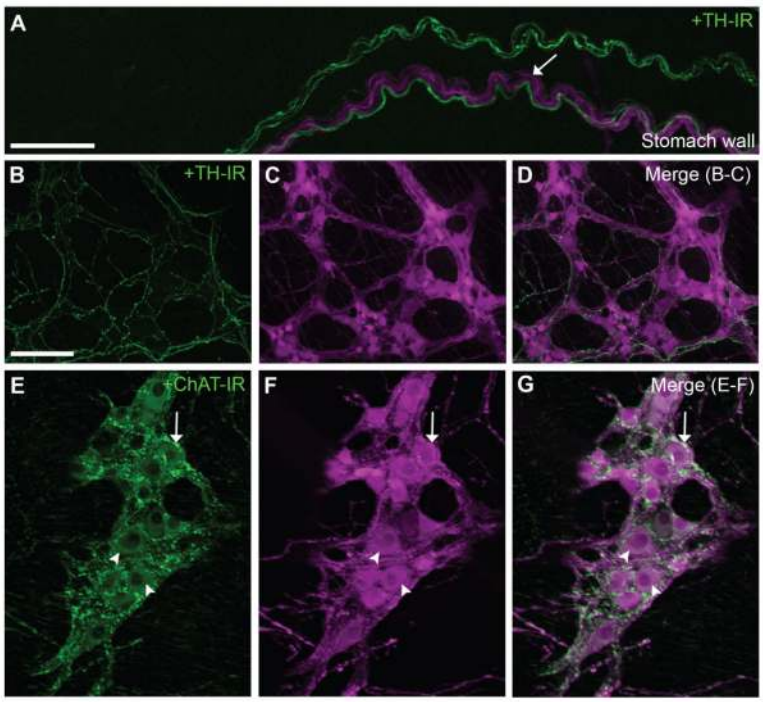

Figure 4.

Immunolabeling of the gastric myenteric plexus with TH and ChAT. **A–D:** TH-positive fibers (green) were found (A) entering the gastric wall (whole mount, 20×, 12 optical plans, 1-μm step), and (B–D) ramifying into the myenteric plexus (whole mount, 10×, 10 optical plans, 11.8-μm step). Note that TdTomato-containing fibers and cell bodies never colocalized with TH immunoreactivity. **E–G:** ChAT immunoreactivity (green) was found in both vagal preganglionic terminals and many myenteric neurons (whole mount, 20×, 9 optical plans, 1-μm step). ChAT was strictly contained in tdTomato-positive fibers and neurons. Nonetheless, the outline of cholinergic fibers and neuronal somas was better revealed by tdTomato fluorescence than ChAT immunoreactivity. Arrows indicate fluorescently labeled neuronal fibers, and arrowheads point to representative cell bodies. Scale bar = 50 μm in A and B (applies to B–G).

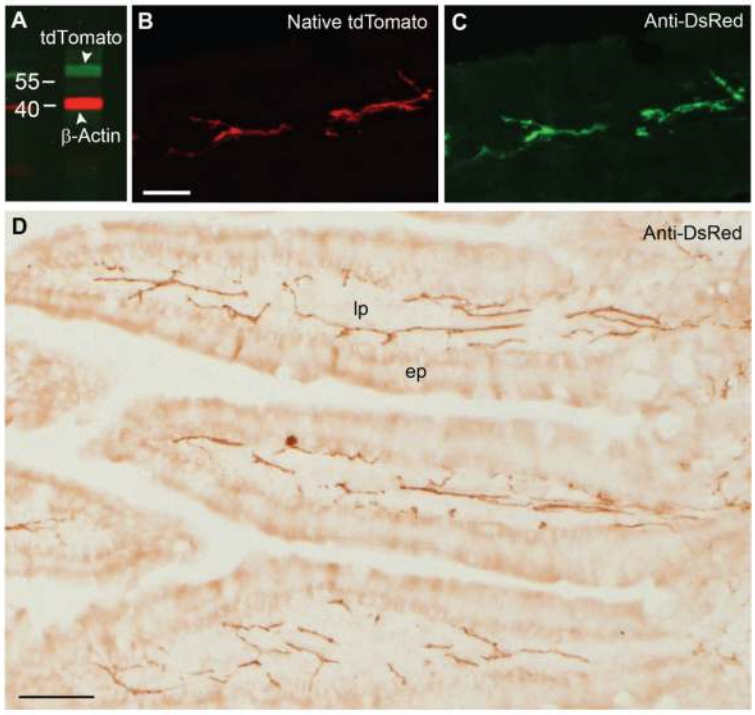

Figure 5.

Western blot analysis and immunohistochemistry for tdTomato. **A:** Immunoblot for tdTomato using a commercially available anti-DsRed antibody, showing a band of 58 kDa (green). The other band corresponds to β-actin (red). Samples were obtained from the duodenum of ChAT-Cre-tdTomato mice, and numbers indicate molecular marker size (kDa). **B,C:** TdTomato-containing fibers in the intestinal mucosa showed bright fluorescence that is directly comparable to that obtained by using the anti-DsRed antibody coupled with Alexa Fluor 488–conjugated secondary antibody (43×, 6 optical plans, 0.87-μm step). **D:** DAB-immunolabeled tdTomato in the intestinal mucosa (20×, brightfield). Abbreviations, ep, epithelium; lp, lamina propria. Scale bar = 20 μm in B (also applies to C); 50 μm in D.

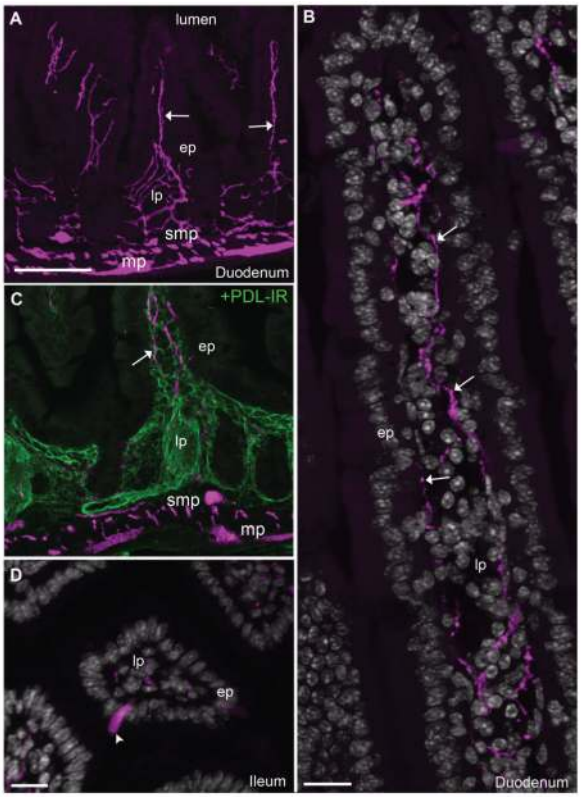

Figure 6.

Innervation to the intestinal mucosa of ChAT-Cre-tdTomato mice. **A:** Abundant innervation was contained within the intestinal lamina propria (10×, 4 optical plans, 7-μm step). **B:** Reconstruction of the mucosa revealed a few individual varicose fibers traveling from the crypt to the tip of villi, sometimes close to the basal laminae or intermingled with cells contained in the middle of the lamina propria (63×, 20 optical plans, 0.5-μm step, 2 tiles). **C:** It must be noted that the observed fibers traveled in close association with the intestinal lymph vasculature (green) contained in the lamina propria (10×, 4 optical plans, 7-μm step). **D:** No fluorescent cells could be found in the mucosa itself with the exception of isolated epithelial cells in the lower intestines (20×, 7 optical plans, 1.62-μm step). In B and D, tissue is labeled with anti-DsRed antibody (magenta) and counterstained with DAPI (white nuclei). Arrows indicate fluorescently labeled neuronal fibers, and arrowheads point to representative cell bodies. Abbreviations: ep, epithelium; lp, lamina propria; mp, myenteric plexus; PDL-IR, podoplanin immunoreactivity; smp, submucosal plexus. Scale bar = 100 μm in A (also applies to C); 20 μm in B and D.

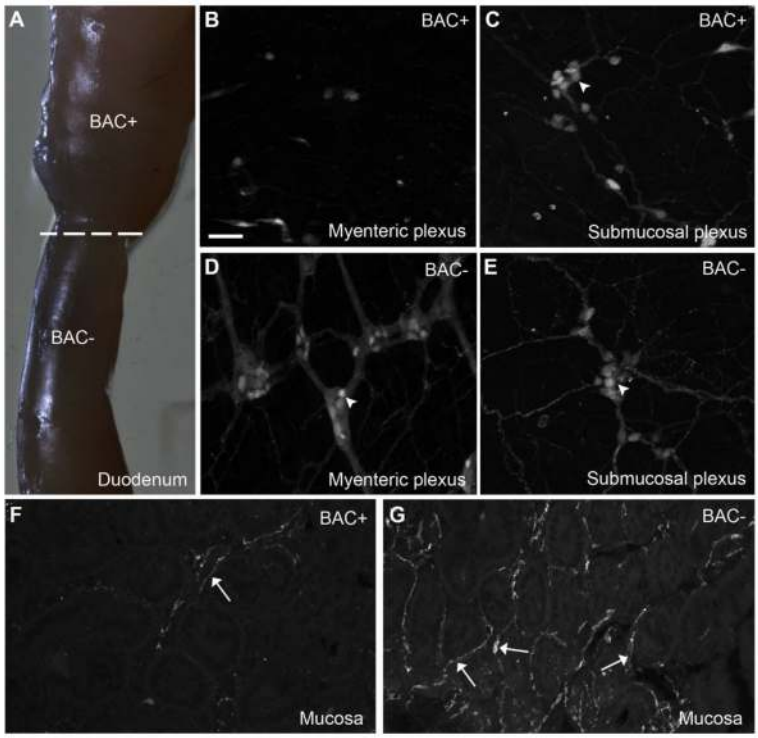

Figure 7.

The innervation to the intestinal mucosa belongs to enteric neurons. **A:** The topical application of benzalkonium chloride onto the duodenum wall results in the swelling of its smooth muscle layers. **B,C:** The segment exposed to the chemical is almost completely devoid of myenteric neurons and preganglionic endings but retained most of its submucosal plexus (whole mount, 10×, 5 optical plans, 1.23-μm step). **D,E:** By comparison, enteric neurons in both layers are intact in the intestines immediately adjacent to the denervated segment. **F,G:** The innervation to the lamina propria of the intestines was largely eliminated in the segment of the intestines exposed to benzalkonium chloride. The remaining fibers could be tracked back to spared submucosal neurons (cryosection, 20×, 5 optical plans, 1.96-μm step). Arrows indicate fluorescently labeled neuronal fibers, and arrowheads point to representative cell bodies. Abbreviations: BAC, benzalkonium chloride. Scale bar = 50 μm in B (applies to B–G).and applies through G. [Color figure can be viewed in the online issue, which is available at wileyonlinelibrary.com.]

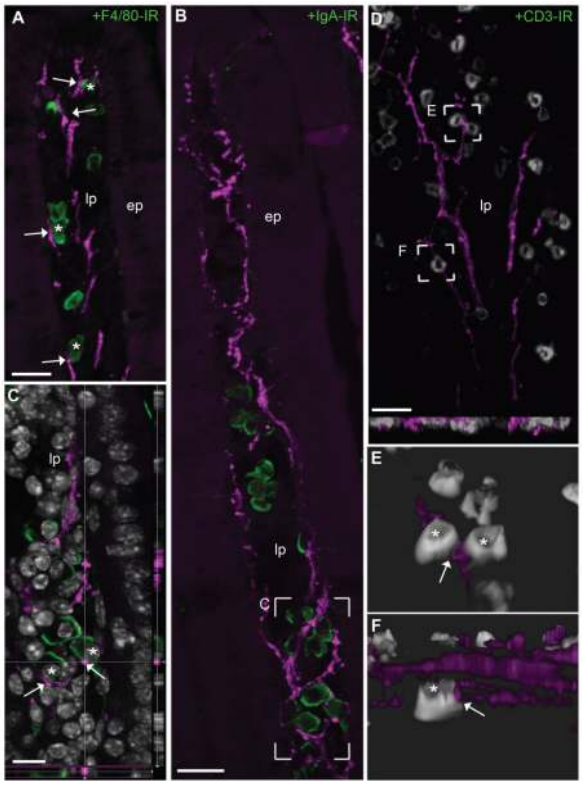

Figure 8.

Proximity of cholinergic fibers and immune cells in the intestinal mucosa. **A–C:** Representative populations of gut immune cells including (A) macrophages (40×, 6 optical plans, 1 μm step), (B) plasma cells (63×, 5 optical plans, 0.71-μm step), and (C) T-cells labeled in the intestines (403×, 20 optical plans, 0.5 μm step, 2 tiles). The examined immune cells (green or white) were frequently approached by individual neuronal fibers. Although our images were collected in the upper intestines (duodenum and jejunum), associations were seen in the entire length of the intestines. **D:** Individual fibers frequently encircled immune cells and approached immune cells very closely (<1 μm or apparent contact in a single plan; 63×, 1 optical plan). In B and C, tissue is labeled with anti-DsRed antibody (magenta) and counterstained with DAPI (white nuclei) **E,F:** Three-dimensional reconstruction was conducted to facilitate the visualization of anatomical associations between immune cells and fibers. Asterisks are positioned over immune cells in close proximity to neuronal fibers, and arrows indicate site of apparent neuroimmune proximity. Abbreviations: CD3-IR, CD 3 immunoreactivity; ep, epithelium; F4/80-IR, F4/80 antigen immunoreactivity; lp, lamina propria; IgA-IR, IgA immunoreactivity. Scale bar = 20 μm in A, B and D; 10 μm in C.

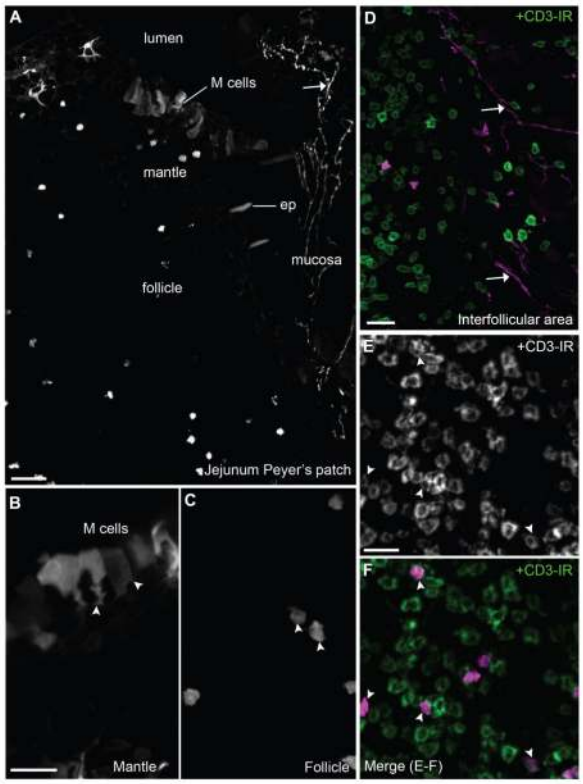

Figure 9.

Cholinergic structures in the Peyer's patches. **A:** Distinct epithelial, immune, and neuronal fluorescent structures were visualized in Peyer's patches. Cells resembling dendritic cells were inconsistently noticed in the dome (10×, 5 optical plans, 5.57-μm step). **B:** Notably, clusters of M cells were seen at the top of the dome (40×, 6 optical plans, 0.68-μm step). These cells display a typical pocket-like structure toward the mantle. **C,D:** Cells resembling lymphocytes were noticed in the follicle (40×, 6 optical plans, 0.68-μm step) and interfollicular areas (20×, 6 optical plans, 1.6-μm step). The innervation to Peyer's patches was confined to the interfollicular areas. **E,F:** CD3 immunoreactivity was frequently found in tdTomato-containing immune cells (40×, 5 optical plans, 0.94-μm step). CD3-positive cells (green or white) are labeled in D, E, and F. Arrows indicate fluorescently labeled neuronal fibers and arrowheads point to representative cell bodies. Abbreviations: ep, epithelium; M cell, microfold cell. Scale bar = 40 μm in A; 20 μm in B (applies to B,C), D, and E (applies to E,F).

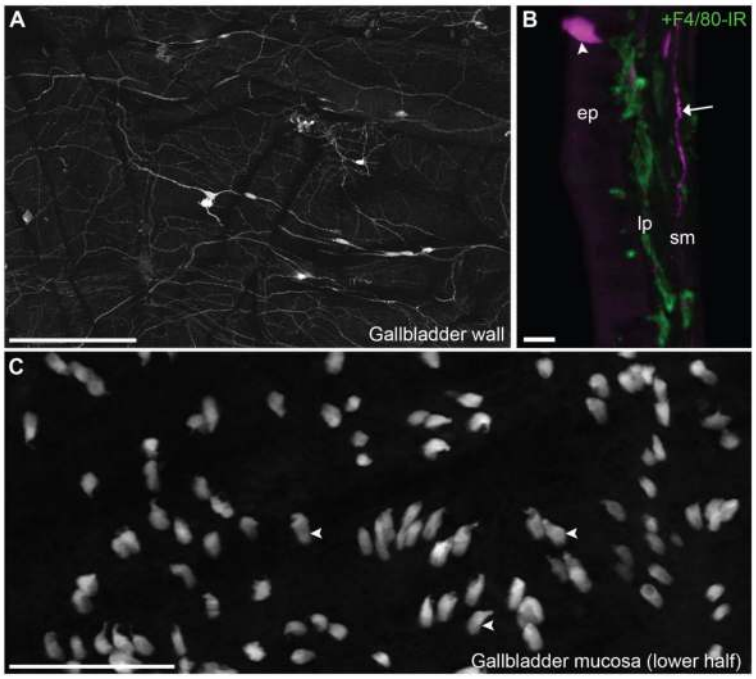

Figure 10.

Cholinergic neuronal and epithelial structures in the gallbladder. **A:** Preganglionic vagal fibers along with postganglionic neurons were visualized in a whole mount of the gallbladder wall (whole mount, 10×, 3 optical plans, 0.62-μm step, 6 tiles). **B:** In a cross section of the gallbladder, it becomes apparent that the gallbladder innervation was confined to the smooth muscle layers but did not penetrate the mucosa (40×, 8 optical plans, 0.9-μm step). However, the thin lamina propria contained many immune cells such as macrophages stained for F4/80 (green). Often, brightly fluorescent cells lodged in the epithelium were observed. **C:** Reconstruction of the gallbladder mucosa (flat mount; basal side facing the observer) revealed the abundance of ChAT-expressing epithelial cells of the gallbladder (whole mount, 20×, 6 optical plans, 0.81-μm step). Their shape was typical of that of brush cells, with an apical protrusion, a bulky cell body, and a thin basal branch. Arrows indicate fluorescently labeled neuronal fibers, and arrowheads point to representative cell bodies. Abbreviations: ep, epithelium; F4/80-IR, F4/80 antigen immunoreactivity; lp, lamina propria; sm, smooth muscle. Scale bar = 400 μm in A; 10 μm in B; 100 μm in C.

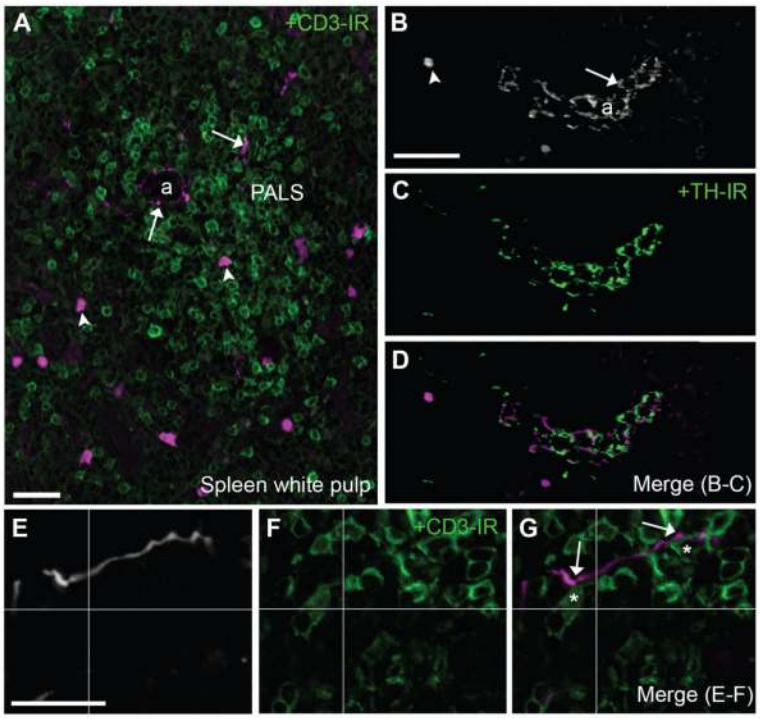

Figure 11.

Identification of neuronal and nonneuronal cholinergic structures in the spleen. **A:** Fluorescent neuronal fibers along with immune cells were found in the splenic white pulp (20×, 7 optical plans, 1-μm step). **B–D:** Varicose TH-positive fibers (green) and putative cholinergic fibers frequently intermingled in periarteriolar areas of the white pulp (20×, 8 optical plans, 0.68-μm step). As in other tissues, tdTomato-containing fibers were never TH immunoreactive. **E–G:** Notably, individual fluorescent fibers were observed around arterioles and occasionally branched into the adjacent periarteriolar lymph sheaths where they contacted CD3-positive cells (green) (40×, 1 optical plan). In E and G, tissue is labeled with an anti-DsRed antibody (white or magenta). Asterisks are positioned over lymphocytes in close proximity to a cholinergic fiber (<1 μm or apparent contact in a single plan). Lastly, isolated immune cells populated the white pulp. Arrows indicate fluorescently labeled neuronal fibers, and arrowheads point to representative cell bodies of immune cells. Abbreviations: a, arteriole; PALS, periarteriolar lymph sheath. Scale bar = 20 μm in A; 50 μm in B (applies to B–D); 10 μm in E (applies to E–F).

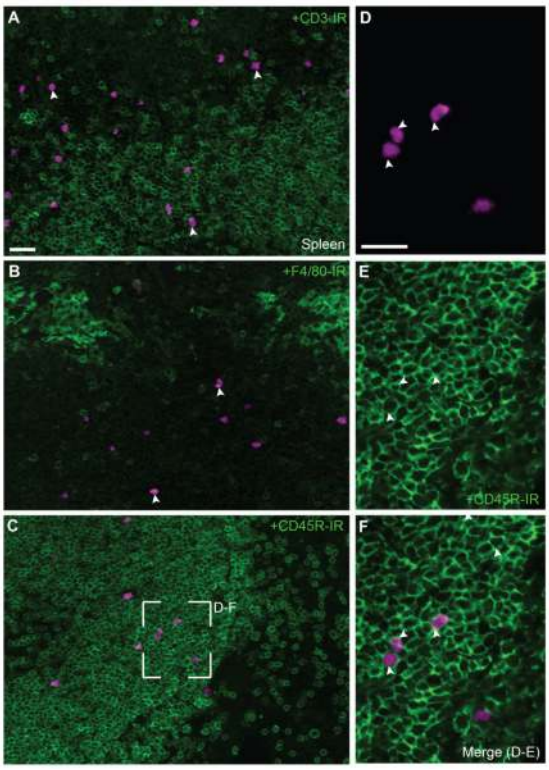

Figure 12.

Phenotyping of immune cells in the spleen. **A:** Although fluorescently labeled immune cells were present in T-cell areas, they rarely colocalized with markers for T-cells (20×, 8 optical plans, 1.48- μm step). **B:** Macrophages stained with F4/80 (green) tended to accumulated in the marginal zone and never colocalized with tdTomato (20×, 8 optical plans, 1.48- μm step). **C:** In contrast, fluorescent immune cells distributed in B-cells areas (20×, 8 optical plans, 1.48- μm step). **D–F:** TdTomato cells were frequently positive for CD45R (403×, 4 optical plans, 0.84- μm step). Of note, markers for immune cells (green) preferentially stained the cell surface rather than the cytoplasm. Arrowheads point to representative cell bodies with cytoplasmic tdTomato. Scale bar = 20 μm in A (applies to A–C); 20 μm in D (applies to D–F).

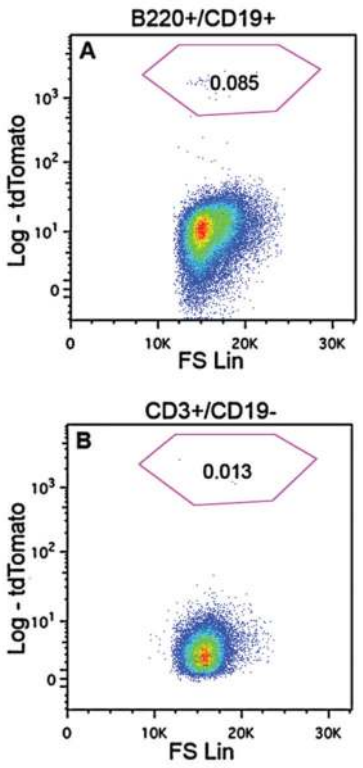

Figure 13.

Flow cytometry analysis of tdTomato-positive lymphocytes. **A:** A small population of splenic B-cells (0.085%), gated as B220+/CD19+, was identified by tdTomato fluorescence. **B:** ChAT positive T-cells were also observed in the spleen, with a small (0.013%) population of CD3e+/CD19− cells expressing tdTomato fluorescence.

TABLE 1

Primary Antisera Used in Immunohistochemistry

Antigen	Immunogen	Manufacturer	Dilution
CD3	20-kDa subunit of the TCR complex clone	eBioscience, cat.14-0032-82, lot. E03447-1630, rat monoclonal (clone 17A2)	1:1,000
ChAT	Human placental enzyme	Millipore, cat.AB144P, lot.23010339, goat polyclonal	1:500
CD45R/B220	Mouse Abelson Leukemia Virus-Induced pre-B tumor cells	eBioscience, cat.17-0452, lot. E07 150-1631, rat monoclonal (clone RA3-6B2)	1:1,000
DsRed and tdTomato	DsRed	ClonTech, cat. 632496, lot. 1202020, rabbit polyclonal	1:1,000–2,000
F4/80	Thioglycollate-stimulated peritoneal macrophages from C57/BL6 mice	AbD Serotec, cat. MCA497, lot. 0710, rat monoclonal (clone CI:A3-1)	1:1,000
IgA	Mouse IgA paraproteins	SouthernBiotech, cat. 1040-01, lot. E7609-R441, goat polyclonal	1:1,000
PDL	Mouse myeloma cell line NS0derived recombinant mouse Podoplanin Gln21-Lys133	R&D Systems, cat. AF3244, lot. WUF0110121, goat polyclonal	1:500
TH	Denatured TH from rat pheochromocytoma	Millipore, cat.AB152, lot.0607034655, rabbit polyclonal	1:2,000

TABLE 2

Relative Abundance of Cholinergic Neuronal Supply and Cholinergic Nonneuronal Cells Within Selected Gut-Associated Lymphoid Tissue, Spleen, and Other Selected Tissues of ChAT-Cre-tdTomato Mice[1]

		Nonneuronal cholinergic cells	
Organs or tissues	**Cholinergic neuronal supply**	**Abundance Phenotype**	
	I. Gut-associated lymphoid tissue		
Gastrointestinal tract			
Wall and submucosa	+++	–	
Epithelium	–	+	Epithelial
Lamina propria[2]	++	–	
Peyer's patches			
Dome	–	+	Microfold cell
Follicle	–	+	T-cell
Interfollicular area[2]	+	+	T-cell
Gallbladder and biliary duct			
Wall	++	–	
Lamina propria	–	–	
Epithelium	–	+ +	Brush cell
	II. Spleen		
Capsule	–	–	
Arterioles	+	–	
Red pulp	–	–	
White pulp[2]	+	+	B- and T-cell
	III. Selected glands and metabolic tissues		
Thyroid gland	++	–	
Salivary glands	+++	–	
Liver parenchyma	–	–	
Pancreas			
Exocrine	++	–	
Endocrine	++	–	
Adrenals			
Medulla	+++	–	
Cortex	–	–	
White adipose tissue			
Mesenteric	–	–	
Perigonadal	–	–	
Brown adipose tissue	–	–	
Sweat glands	++	–	
Testis			
Capsule	–	–	
Parenchyma	–	–	

		Nonneuronal cholinergic cells	
Organs or tissues	**Cholinergic neuronal supply**	**Abundance Phenotype**	
Airways			
Epithelium	–	+ / –	Epithelial
Lamina propria	+/–	–	
Smooth muscle	+++	–	
Skeletal muscle	++	–	
	IV. Selected large blood vessels		
Aortic arch	++	–	
Abdominal aorta	++	–	
Portal vein (hilus)	++	–	
Hepatic artery (hilus)	++	–	
Mesenteric arteries and veins	++	–	
Skin arteries	++	–	
Pulmonary arteries	++	–	
Coronary arteries	++	–	

[1] Estimates are based on the survey of three different animals. Based on morphological criteria, double-labeling, and flow-sorting experiments, we further narrowed down the cellular identity of nonneuronal cells, as indicated in the right column. Of note, the abundance of neuronal somas (postganglionic neurons) in the periphery is not included in this survey. Estimates: +++, high density; ++, moderate density; +, low density; –, absence of fluorescence.

[2] Close proximity (<1 μm or apparent contact) between cholinergic fibers (tdTomato fluorescent) and immune cells.